Therapeutic effect of balloon-occluded retrograde transvenous obliteration for gastric varices in relation to haemodynamics in the short gastric vein

[1]H OKUGAWA, MD, [1]H MARUYAMA, MD, [1]S KOBAYASHI, MD, [1]H YOSHIZUMI, MD, [2]S MATSUTANI, MD and [1]O YOKOSUKA, MD

[1]*Department of Medicine and Clinical Oncology, Chiba University Graduate School of Medicine, 1-8-1, Inohana, Chuou-ku, Chiba, 260-8670 and* [2]*Chiba College of Health Science, 2-10-1, Wakaba, Mihama-ku, Chiba 261-0014, Japan*

ABSTRACT. The aim of this study was to elucidate the relationship between the therapeutic effect of balloon-occluded retrograde transvenous obliteration (B-RTO) and haemodynamic features in the short gastric vein (SGV) in patients with gastric fundal varices (GV). The subjects in this retrospective cohort study comprised 34 patients who had moderate- or large-grade GV with the SGV both on retrograde venography and Doppler ultrasound. The diameter, flow velocity and flow volume in the SGV measured by Doppler ultrasound before B-RTO with 1 h balloon occlusion were compared with the therapeutic effect. Embolisation of GV was achieved in 30/34 patients (88.2%): 27 by initial B-RTO and 3 by second B-RTO. Flow velocity and flow volume in the SGV before B-RTO were significantly lower in the 27 patients with a complete effect on initial B-RTO (7.19 ± 2.44 cm s^{-1}, $p=0.0246$; 189.52 ± 167.66 ml min^{-1}, $p=0.002$) than in the 7 patients with an incomplete effect (10.41 ± 5.44 cm s^{-1}, 492.14 ± 344.94 ml min^{-1}). Neither endoscopy nor contrast-enhanced CT had recurrent findings of GV in the subject during the follow-up period (94–1440 days; mean, 487.2 ± 480.5 days). In conclusion, haemodynamic evaluation of the SGV using Doppler ultrasound may be useful for the prediction of the therapeutic effect of B-RTO.

Received 16 November 2008
Revised 31 January 2009
Accepted 3 February 2009

DOI: 10.1259/bjr/28956799

Gastric varices are one of the haemodynamic features of major potential consequence in patients with portal hypertension. The incidence of gastric varices is reported to be approximately 20–25% [1–3], which is lower than that of oesophageal varices (EV). Furthermore, lower bleeding rates of gastric varices than those of EV have been described in previous studies [1, 4]. However, those studies have shown that the mortality rate caused by bleeding from gastric fundal varices (GV) is in the range of 25–55% [1–5]. Therefore, management of bleeding GV is vital in the clinical practice of patients with portal hypertension.

In 1991, Kanagawa et al [6] introduced a new technique — balloon-occluded retrograde transvenous obliteration (B-RTO) — for the treatment of GV. It is a simple and effective procedure for the embolisation of GV, and previous studies reported the complete eradication of GV in over 78% of patients, with a low rate of recurrence [6–9]. However, this technique does have some intractable cases, reportedly 12.5–40% [6, 8–10], the reason for which has not been fully discussed. High-flow volume in the GV may account for the incomplete effect of B-RTO.

It was reported that over 50% of GV have short gastric vein (SGV) and/or posterior gastric vein (PGV) dominant, and about 25% of GV have left gastric vein (LGV) dominant, blood supply on portograms [11], and that Doppler ultrasound could evaluate the haemodynamics in these gastric veins [12, 13]. As the SGV is one of the major inflow routes for GV, its haemodynamics might be related to the pathophysiology of GV and the therapeutic effect of GV after B-RTO. Based on this hypothesis, we examined the haemodynamics in the SGV using Doppler ultrasound before B-RTO. The purpose of the present study was to elucidate the relationship between the therapeutic effect of B-RTO for GV and the haemodynamic features in the SGV.

Methods and materials

Patients

83 consecutive patients (36 female, 47 male; age range, 42–80 years; mean, 62.6 ± 9.42 years) with GV were treated with B-RTO between March 1998 and September 2006 in our department. Among them, 34 patients (14 female, 20 male; age range, 46–80 years; mean, 63.6 ± 8.95 years) were enrolled in this retrospective cohort study, according to both of the following two criteria: (i) the SGV was demonstrated by retrograde venography via GV (56/83, 67.5%); (ii) detection and blood flow measurement in the SGV was conducted by Doppler ultrasound in patients who had SGV on the venogram (34/56, 60.7%). Informed written consent for B-

Address correspondence to: Hitoshi Maruyama, Department of Medicine and Clinical Oncology, Chiba University Graduate School of Medicine, 1-8-1, Inohana, Chuou-ku, Chiba 260-8670, Japan. E-mail: maru-cib@umin.ac.jp

Table 1. Clinical background of patients treated by B-RTO (n=34)

Sex (male/female)	20/14
Age (years): mean ± SD (range)	63.6±8.95 (46–80)
Application electively/prophylactically	17/17
Liver disease	
LC	33
Alcohol	8
HCV	17
HBV	2
Primary biliary cirrhosis	1
Cryptogenic	5
Chronic hepatitis	1
Cryptogenic	1
Child–Pugh class A/B	18/15
Presence of hepatocellular carcinoma	13
Form of gastric varices F1/F2/F3	0/25/9
Presence of oesophageal varices before B-RTO	17
Form of oesophageal varices F1/F2/F3	11/5/1

B-RTO, balloon-occluded retrograde transvenous obliteration; SD, standard deviation; LC, liver cirrhosis; F1, small straight; F2, enlarged tortuous; F3, large coil-shaped; HBV, hepatitis B virus; HCV, hepatitis C virus.

RTO was obtained from all patients, and the research was carried out in accordance with the Helsinki Declaration. The ethics committee in our hospital deemed this retrospective study as appropriate for publication.

33 patients had liver cirrhosis and one had chronic hepatitis. Diagnosis of liver cirrhosis was based on imaging modalities with laboratory data and clinical presentation, and diagnosis of chronic hepatitis was based on percutaneous liver biopsy. The cause of liver diseases was hepatitis B virus infection in 2 patients, hepatitis C virus infection in 17, alcohol abuse in 8, primary biliary cirrhosis in 1, and cryptogenic in 6. Hepatic functional reserve in cirrhotic patients according to the Child–Pugh classification was A in 18 patients and B in 15 patients [14]. 13 patients had hepatocellular carcinoma (HCC), which was controlled by non-surgical treatment, and none had portal venous tumour thrombus or portal venous thrombus (Table 1).

Endoscopy

GV were diagnosed by endoscopic examination in all patients. The form of GV was evaluated according to the general rules of the Japanese Society for Portal Hypertension [15]: small straight (mild grade, F1); enlarged tortuous (moderate grade, F2); or large coil-shaped (large grade, F3). 25 patients had F2 and 9 had F3. 17 of the 34 patients had bleeding histories that were confirmed by endoscopic examination: 10 with active bleeding on endoscopic findings and 7 with a bleeding history, having inactive bleeding with no other cause for gastrointestinal bleeding. 10 patients with active bleeding received endoscopic treatment to attain haemostasis before B-RTO: endoscopic variceal ligation (EVL) in 1 patient; endoscopic cyanoacrylate injection in 7 patients; both EVL and endoscopic cyanoacrylate injection in 1 patient; and endoscopic clipping following cyanoacrylate injection in 1 patient. The remaining 17 patients had no bleeding history, haematemesis or melena during their clinical course.

17 patients also had EV: 11 with F1, 5 with F2 and 1 with F3. A prophylactic treatment for EV was performed in one patient with F2 varices before B-RTO and one patient with F1 varices after B-RTO. Follow-up endoscopy was performed approximately every 6 months after B-RTO.

B-RTO

The application of B-RTO in our study constituted elective treatment in 17 patients ("bleeders") and prophylactic treatment in 17 patients who wished to receive it. All patients had a gastrorenal shunt placed for the drainage pathway from the GV by ultrasound/CT [16]. Initially, a 6F balloon catheter (Selecon MP catheter; Clinical Supply, Gifu, Japan) was inserted into the drainage route of the GV (a gastrorenal shunt). Then, retrograde venography was performed under balloon inflation to confirm the demonstration of both the GV and the inflow routes. Subsequently, the sclerosing agent prepared with equal amounts of 10% ethanolamine oleate (Oldamin; Mochida Pharmaceutical, Tokyo, Japan) and iopamidol (Iopamiron 300; Nihon Schering, Osaka, Japan) was injected in a retrograde manner under fluoroscopy to fill both the GV and the inflow routes. After ~1 h, as much of the agent as possible was withdrawn and the balloon catheter was removed. Blood pressure, pulse rate, electrocardiogram, arterial oxygen saturation and urine volume were monitored during the treatment, and 4000 units of haptoglobin (Green Cross, Osaka, Japan) was administered intravenously to prevent renal failure potentially induced by ethanolamine oleate. The therapeutic effect was evaluated by contrast-enhanced CT within 1 week after B-RTO, and therapeutic success was defined as absence of contrast enhancement in the GV on CT images. B-RTO was performed 1 week or 2 weeks after the previous B-RTO in cases of an incomplete embolisation effect in the GV. All B-RTO procedures were performed by H.M. and H.O.

Doppler ultrasound examination

Doppler ultrasound was performed using SSA-390A or SSA-770A systems (Toshiba, Tokyo, Japan) with a

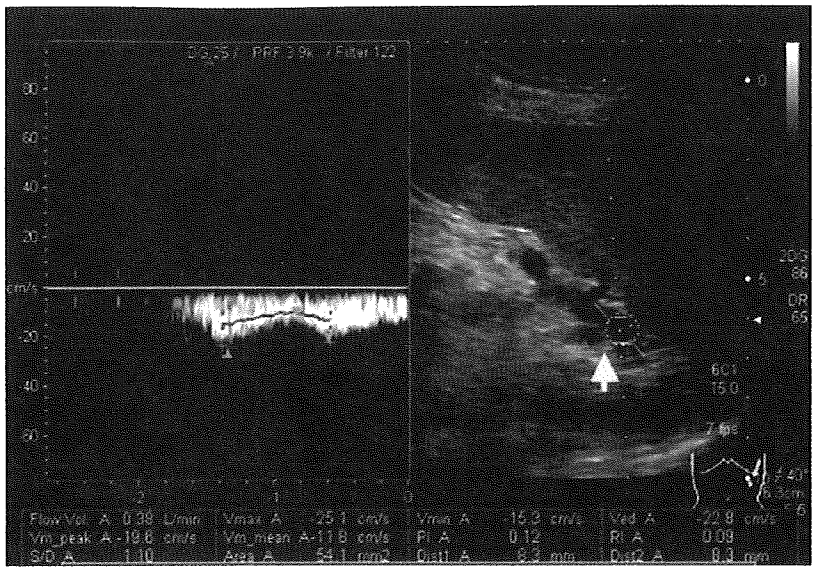

Figure 1. Doppler ultrasound of patients with gastric fundal varices. The sonogram under the left intercostal scan demonstrated the short gastric vein (SGV) with flow in the hepatofugal direction (arrow).

3.75 MHz convex probe before B-RTO. All patients underwent ultrasound examinations, after an overnight fast except for the bleeding cases, in the supine position and in an intermediate or light inspiratory phase of respiration. Among the 10 patients who received endoscopic treatments to attain haemostasis, Doppler ultrasound examination was applied emergently just before the endoscopic treatments in five bleeders and after the endoscopic treatment in the other five bleeders. The SGV was demonstrated by a left inter- or sub-costal scan around the splenic hilum (Figure 1) [12]. The beam–vessel angle was less than 60° in every patient, and the diameter (mm), flow velocity (cm s^{-1}) and mean flow volume (ml min^{-1}) of the SGV were measured by grey-scale ultrasound and the pulsed Doppler method. Doppler ultrasound was performed by H.M. (n=25) or S.M. (n=9), who were hepatologists with over 8 years of experience of ultrasound examinations at the time of the initial case. Observer variability was obtained in 12 patients by independent measurements strictly performed by two operators for interobserver variability and by one operator for intraobserver variability on the same day. The average value was used for SGV data in these 12 cases. All of the ultrasound images for the SGV were carefully reviewed by H.O. to confirm that the fast Fourier transform analysis was conducted under appropriate measurement conditions.

Contrast-enhanced CT

Contrast-enhanced CT with dynamic study was performed using Vertex 3000 Formula (GE Yokogawa Medical Systems, Hino, Japan) or Lightspeed ultra16 (GE Yokogawa Medical Systems) equipment. Iodinated contrast medium (Iopamiron 300; Nihon Schering, Osaka, Japan) was injected at 3 ml s^{-1} with a total dose of 100 ml from the antecubital vein by mechanical power injector, and scanning was performed with a 30 s delay between contrast medium administration and the start of imaging for the hepatic artery-dominant phase, a 80 s delay for the portal vein-dominant phase, and a 180 s delay for the equilibrium phase. Contrast-enhanced CT was performed before B-RTO, within 1 week after the treatment and approximately every 6 months during follow-up observation. The therapeutic effect was assessed by S.K. as the presence or absence of the contrast-enhanced findings at the variceal area.

Statistical analysis

The results in this study were expressed as mean ± standard deviation (SD). Statistical analysis was performed by Stat View-J 5.0 statistical software (Abacus Concepts, Berkeley, CA). The relationship between the therapeutic effect of B-RTO and the haemodynamics in the SGV was analysed using the Student's t-test. The interobserver or intraobserver variability was obtained as a coefficient of variation, calculated by dividing the standard deviation by the mean and multiplying by 100. p-values <0.05 were considered to be statistically significant.

Results

Embolisation effect of B-RTO

Initial B-RTO completely embolised GV in 27 of the 34 patients (79.4%), with the other 7 showing an incomplete effect. Three of the seven patients had complete embolisation effects after a second B-RTO, and another one had complete embolisation after a third B-RTO combined with percutaneous transhepatic obliteration. No additional treatment was added for the remaining three patients who declined further intervention. Therefore, B-RTO achieved an embolisation effect in 30 of the 34 patients (88.2%). 6 months after B-RTO, endoscopy showed a disappearance or decrease in size of the GV, and contrast-enhanced CT did not show any enhancement at the variceal site. Subsequently, neither endoscopy nor contrast-enhanced CT showed recurrent findings of GV in the subject during the follow-up period (94–1440 days; mean, 487.2±480.5 days). Fever (>37.5℃; 21/34 patients, 61.8%), haemoglobinuria

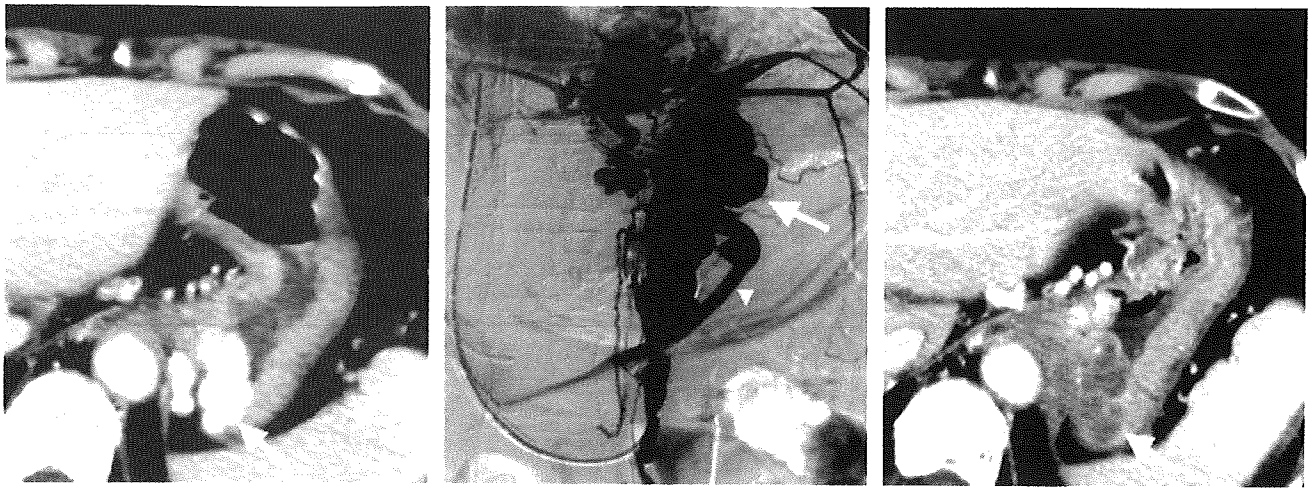

(a) (b) (c)

Figure 2. Gastric fundal varices (GV) before and after balloon-occluded retrograde transvenous obliteration (B-RTO) in a 72-year-old woman with chronic hepatitis (cryptogenic). (a) Contrast-enhanced CT before B-RTO showing the GV (arrow); (b) retrograde venography from a gastrorenal shunt showing the GV (arrow) and short gastric vein (SGV; arrowhead); (c) contrast-enhanced CT after B-RTO (contrast enhancement was not observed at the variceal site (arrow)). This case was completely treated by the initial B-RTO. Diameter, flow velocity and flow volume of the SGV on Doppler ultrasound were 6.9 mm, 6.3 cm s^{-1} and 140 ml min^{-1}, respectively.

(27/34, 79.4%) and pain (13/34, 38.2%) were found as short-term complications.

Haemodynamics of the SGV before B-RTO in relation to the therapeutic effect

The SGV had hepatofugal flow direction on Doppler sonograms in all patients before B-RTO. Flow velocity and flow volume in the vessel before B-RTO were significantly lower in the 27 patients who were completely treated by the initial B-RTO (7.19 ± 2.44 cm s^{-1}, $p=0.0246$; 189.52 ± 167.66 ml min^{-1}, $p=0.002$; Figure 2) than in the 7 patients who required two or three sessions (10.41 ± 5.44 cm s^{-1}, 492.14 ± 344.94 ml min^{-1}). The diameter of the SGV was smaller in the former (6.46 ± 2.37 mm) than in the latter (8.07 ± 2.42 mm) group, but the difference was not statistically significant ($p=0.121$; Figure 3). Interobserver variability was $12.8 \pm 10.1\%$ and intraobserver variability was $4.7 \pm 4.1\%$ for the Doppler measurement data. 10 patients who received endoscopic treatments before B-RTO were treated by initial B-RTO alone. There was no significant difference between the therapeutic effect of B-RTO and clinical backgrounds such as bleeding history, presence of HCC or Child–Pugh classification.

Discussion

The management of bleeding GV is critical in the clinical practice of patients with portal hypertension [1–5]. Recent developments in medical technologies have resulted in the improvement of therapeutic outcome in patients with GV, and the greater application of B-RTO may be the most noteworthy advancement [6–10].

As shown by our results, GV were completely embolised in 30/34 patients (88.2%): 27 patients by initial 1-h B-RTO and 3 patients by a second 1-h B-RTO, which is similar to results from previous studies [6, 8–10]. In addition, there were neither serious complications nor recurrent cases during the observation period. Although 1 h was thought to be a time that patients could easily tolerate in the supine position under local anaesthesia alone, it is true that this selection of procedure duration was not based on scientific evidence. However, as our method could achieve sufficient therapeutic effect in the majority of patients with moderate- or large-grade GV, the results from this study might help the standardisation of the B-RTO method. Additionally, the optimum occlusion time to achieve complete embolisation should be examined in cases with a highly developed SGV before B-RTO as a tailor-made treatment.

A single session of 1 h B-RTO did not provide complete embolisation in 7/34 (20.6%) of the GV patients. Flow velocity and flow volume in the SGV were significantly higher in these treatment-resistive cases than in cases completely treated after a single session. Meanwhile, there was no significant difference between the results of embolisation of GV and the clinical backgrounds, such as bleeding history, presence of HCC and degree of liver damage. Therefore, it is suggested that the therapeutic effect of 1 h B-RTO may depend on the pre-treatment haemodynamics of the SGV, a major inflow route for GV. Indeed, all 10 patients who received endoscopic treatment before B-RTO had complete embolisation of their GV after a single session; this might be caused by decreased blood flow in the SGV as a result of the endoscopic treatments prior to B-RTO. Although the SGV in such patients had treatment-modified haemodynamics before B-RTO, candidates for B-RTO of GV may include a certain number of these patients in clinical practice. As the purpose of our study was to examine the relationship between the therapeutic effect of B-RTO and haemodynamics in the SGV before

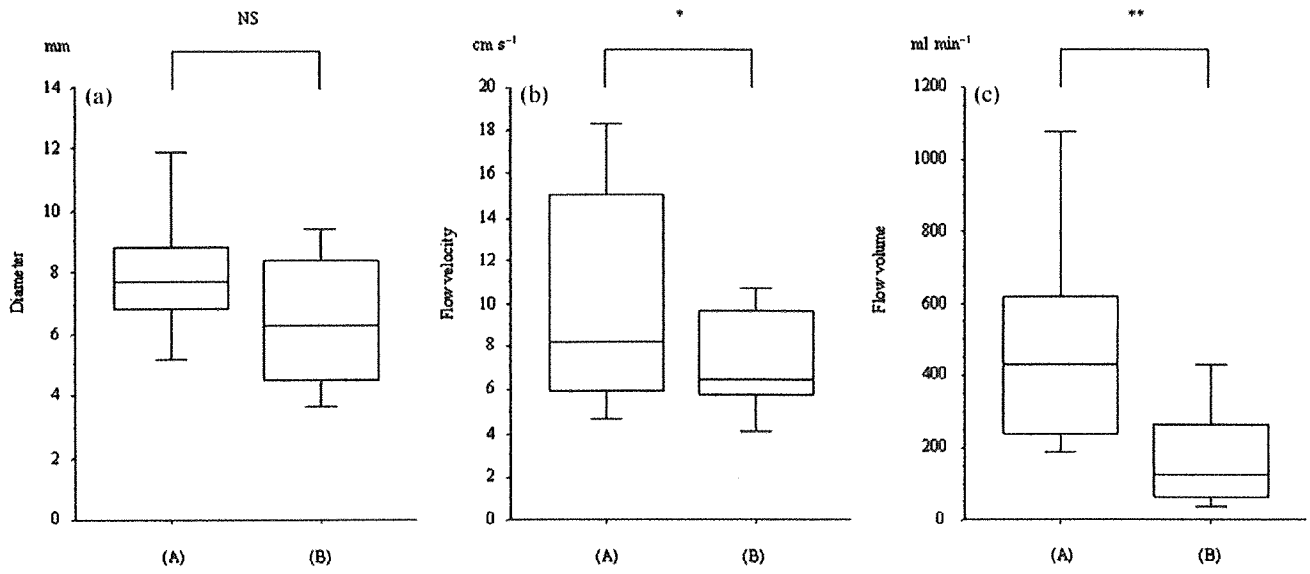

Figure 3. Relationship between the effect of balloon-occluded retrograde transvenous obliteration (B-RTO) and the haemodynamics of the short gastric vein (SGV) before treatment: (a) diameter, (b) flow velocity and (c) flow volume. (A) Patients incompletely treated by the initial B-RTO (n=7); and (B) patients completely treated by the initial B-RTO (n=27). Flow velocity and flow volume in the SGV before B-RTO were significantly lower in the 27 patients completely treated by initial B-RTO than in the 7 patients incompletely treated by initial B-RTO. Data were expressed by box-and-whisker plots. The top and bottom of the box indicate upper and lower quartiles, respectively, and the horizontal line in the box represents the median value. The two horizontal lines outside the box (whisker) indicates the smallest and largest non-outlier observation. *,** $p< 0.05$ (Student's t-test). NS, not significant.

B-RTO, the presence or absence of precedent endoscopic treatment might be trivial. Nevertheless, the evaluation of haemodynamics in the SGV by Doppler ultrasound before B-RTO may be predictive for the embolisation of GV.

There are few studies on the ultrasound findings of SGVs in the literature. The previous work reported a poor detectability of 10%, which may be caused by low performance of ultrasound equipment 20 years ago and/or the study subjects with portal hypertension not being limited to patients with moderate- or large-grade GV, as in our study [12]. Meanwhile, the SGV was detected and the blood flow was measured by ultrasound in 60.7% patients who had a SGV on the venogram in our study. Nowadays, Doppler ultrasound could be one of the tools used to assess the haemodynamics in the SGV that might reflect the pathophysiology of patients with GV.

Endoscopic cyanoacrylate injection is effective for the treatment of bleeding gastric varices. However, it does not necessarily provide sufficient long-term protection against GV bleeding, and previous reports have shown a cumulative rebleeding rate from 18–33% per year after cyanoacrylate injection [17, 18]. Therefore, the application of endoscopic treatment alone as a curative treatment for bleeding GV may be insufficient, and subsequent additional treatment, such as B-RTO, may be required. An appropriate timing of elective B-RTO after the haemostasis by endoscopic treatment should be established in the near future.

There were some limitations to our study. The first is that the therapeutic effect of B-RTO in the present study was compared with the haemodynamics in the SGV alone. As other collateral vessels, such as the LGV and/or PGV, are also inflow routes into GV in some cases [11], the haemodynamics of these vessels might be involved with the therapeutic effect of B-RTO. The next is that our data lack values of portal venous pressure, which might be associated with the embolisation effect of GV. Although the previous study has shown that portal venous pressure is not always high in patients with GV owing to the development of a gastrorenal shunt [11], B-RTO increases the portal venous pressure by embolisation of the variceal route [19]. The relationship between portal venous pressure and the therapeutic effect of B-RTO remains to be solved in further studies. Thirdly, our results were obtained in a retrospective study. The embolisation effect of B-RTO needs to be confirmed according to the haemodynamics in the SGV on Doppler ultrasound in prospective studies with large number of patients.

In conclusion, 1 h B-RTO may be a promising treatment method for moderate- to large-grade GV and could provide sufficient embolisation. Pre-treatment evaluation of portal haemodynamics by Doppler ultrasound might be predictive for the therapeutic effect of this technique.

References

1. Sarin SK, Sachdev G, Nanda R, Misra SP, Broor SL. Endoscopic sclerotherapy in the treatment of gastric varices. Br J Surg 1988;75:747–50.
2. Sarin SK, Lahoti D, Saxena SP, Murthy NS, Makwana UK. Prevalence, classification and natural history of gastric varices: a long-term follow-up study in 568 portal hypertension patients. Hepatology 1992;16:1343–9.
3. Kim T, Shijo H, Kokawa H, Tokumitsu H, Kumara K, Ota K, et al. Risk factors for hemorrhage from gastric fundal varices. Hepatology 1997;25:307–12.
4. Trudeau W, Prindiville T. Endoscopic injection sclerosis in bleeding gastric varices. Gastrointest Endosc 1986;32:264–8.

5. Akiyoshi N, Shijo H, Iida T, Yokoyama M, Kim T, Ota K, et al. The natural history and prognostic factors in patients with cirrhosis and gastric fundal varices without prior bleeding. Hepatol Res 2000;17:145–55.
6. Kanagawa H, Mima S, Kouyama H, Gotoh K, Uchida T, Okuda K. Treatment of gastric fundal varices by balloon occluded retrograde transvenous obliteration. J Gastroenterol Hepatol 1996;11:51–8.
7. Koito K, Namieno T, Nagakawa T, Morita K. Balloon-occluded retrograde transvenous obliteration for gastric varices with gastrorenal or gastrocaval collaterals. AJR Am J Roentgenol 1996;167:1317–20.
8. Hirota S, Matsumoto S, Tomita M, Sako M, Kono M. Retrograde transvenous obliteration of gastric varices. Radiology 1999;211:349–56.
9. Chikamori F, Kuniyoshi N, Shibuya S, Takase Y. Eight years of experience with transjugular retrograde obliteration for gastric varices with gastrorenal shunt. Surgery. 2001;129:414–20.
10. Fukuda T, Hirota S, Sugimura K. Long-time results of balloon-occluded retrograde transvenous obliteration for the treatment of gastric varices and hepatic encephalopathy. J Vasc Interv Radiol 2001;12:327–36.
11. Watanabe K, Kimura K, Matsutani S, Ohto M, Okuda K. Portal hemodynamics in patients with gastric varices: a study of 230 patients with esophageal and gastric varices using portal vein catheterization. Gastroenterology 1988;95:434–40.
12. Dokmeci AK, Kimura K, Matsutani S, Ohto M, Ono T, Tsuchiya Y, et al. Collateral veins in portal hypertension: demonstration by sonography. AJR Am J Roentgenol 1981;137:1173–8.
13. Matsutani S, Furuse J, Ishii H, Mizumoto H, Kimura K, Ohto M. Hemodynamics of the left gastric vein in portal hypertension. Gastroenterology 1993;105:513–8.
14. Pugh RN, Murray-Lyon IM, Dawson JL, Pietroni MC, Williams R. Transection of oesophagus for bleeding oesophageal varices. Br J Surg 1973;60:646–9.
15. The general rules for study of portal hypertension. 2nd edn. The Japan Society for Portal Hypertension. Tokyo: Kanehara, 2004:51–9.
16. Maruyama H, Okugawa H, Yoshizumi H, Kobayashi S, Yokosuka O. Hemodynamic features of gastrorenal shunt: a Doppler study in cirrhotic patients with gastric fundal varices. Acad Radiol 2008;15:1148–54.
17. Sarin SK, Jain AK, Jain M, Gupta R. A randomized controlled trial of cyanoacrylate versus alcohol injection in patients with isolated fundic varices. Am J Gastroenterol 2002;97:1010–5.
18. Akahoshi T, Hashizume M, Shimabukuro R, Tanoue K, Tomikawa M, Okita K, et al. Long-term results of endoscopic histoacryl injection sclerotherapy for gastric variceal bleeding. A 10-year experience. Surgery 2002;131:S176–81.
19. Akahane T, Iwasaki T, Kobayashi N, Tanabe N, Takahashi N, Gama H, et al. Changes in liver function parameters after occlusion of gastrorenal shunt with balloon-occluded retrograde transvenous obliteration. Am J Gastroenterol 1997;92:1026–30.

Research Article

EASL EUROPEAN ASSOCIATION FOR THE STUDY OF THE LIVER | JOURNAL OF HEPATOLOGY

Association between mutations in the core region of hepatitis C virus genotype 1 and hepatocellular carcinoma development

Shingo Nakamoto, Fumio Imazeki*, Kenichi Fukai, Keiichi Fujiwara, Makoto Arai, Tatsuo Kanda, Yutaka Yonemitsu, Osamu Yokosuka

Department of Medicine and Clinical Oncology, Graduate School of Medicine, Chiba University, 1-8-1 Inohana, Chuo-Ward, Chiba City, Chiba 260-8670, Japan

Background & Aims: To determine whether amino acid mutations in the core region of hepatitis C virus (HCV) genotype 1 are associated with response to interferon (IFN) therapy and development of hepatocellular carcinoma (HCC).

Methods: We followed up 361 patients (median duration, 121 months), and IFN monotherapy was administered to 275 (76%) [sustained virological response (SVR) rate, 26.5%]. Using pretreatment sera, mutations at core residues 70 and 91 were analyzed [double wild (DW)-type amino acid pattern: arginine, residue 70; leucine, residue 91].

Results: A low aspartate aminotransferase (AST)/alanine aminotransferase (ALT) ratio and low HCV load were independently associated with SVR, but core mutations were not. During follow-up, 12 of 81 (14.8%) patients with the DW-type pattern and 52 of 216 (24.1%) patients with non-DW-type pattern developed HCC ($p = 0.06$, Breslow–Gehan–Wilcoxon test). Multivariate analysis with the Cox proportional-hazards model revealed the following independent risk factors for HCC: male gender [$p < 0.0001$; risk ratio (RR), 3.97], older age ($p < 0.05$; RR, 2.08), advanced fibrosis ($p < 0.0001$; RR, 5.75), absence of SVR ($p < 0.01$; RR, 10.0), high AST level ($p < 0.01$; RR, 2.08), high AST/ALT ratio ($p < 0.01$; RR, 2.21), and non-DW-type pattern ($p < 0.05$; RR, 1.96). In patients with F0–F2 fibrosis at entry, non-DW-type was likely to lead to cirrhosis ($p = 0.051$).

Conclusions: In HCV genotype 1 patients, HCC risk could be predicted by studying core mutations, response to IFN, and host factors like age, gender, and liver fibrosis.

Introduction

Hepatitis C virus (HCV) infection is a global health problem and the number of chronic carriers worldwide is estimated at 170 million [1]. HCV causes chronic hepatitis, which may progress to liver cirrhosis and hepatocellular carcinoma (HCC); the speed of disease progression, though, varies among patients [2,3]. Age, gender, steatosis, liver fibrosis, and response to interferon (IFN) therapy are reported to be associated with disease progression and HCC development [4–7]. HCV has six major genotypes, of which genotype 1 is most common in Japan and reported to be associated with increased severity and progression of chronic liver disease [8,9]. HCV contributes to HCC by directly modulating the pathways promoting the malignant transformation of hepatocytes [10–13]. Studies on transgenic mice revealed that the HCV core protein has oncogenic potential [14], but other studies yielded conflicting results [15,16]. Recently, mutations at amino acids 70 and 91 in the core region were shown to predict virological response to therapy with IFN plus ribavirin and also HCC development [17–19]. However, few studies support these results, and hence, the clinical impact of core mutations on HCC development is still unclear. In order to determine the viral factors associated with HCC development, we performed a retrospective cohort study on 361 patients with chronic liver disease caused by HCV genotype 1 infection and analyzed the amino acids present at core residues 70 and 91. Additionally, we evaluated whether these mutations were associated with IFN treatment, cirrhosis development, or host factors like age and gender.

Patients and methods

Study population

We enrolled 361 consecutive HCV genotype 1-infected patients who had undergone liver biopsy between August 1986 and June 1998 at Chiba University Hospital. At the enrollment time, the absence of HCC was proven by abdominal ultrasonography (US), computed tomography (CT), or magnetic resonance imaging (MRI). All the patients tested positive for anti-HCV antibody, determined by second-generation enzyme-linked immunosorbent assay. Patients with chronic hepatitis B, autoimmune hepatitis, primary biliary cirrhosis, hemochromatosis, Wilson disease, or alcoholic liver disease were excluded, as were patients with a history of alcoholism, drug abuse, or IFN therapy. Written informed consent was obtained from all patients before performing liver biopsy.

Keywords: Hepatitis C virus; Core region; Hepatocellular carcinoma; Interferon; Sustained virological response.

Received 30 April 2009; received in revised form 22 July 2009; accepted 4 August 2009; available online 23 October 2009

* Corresponding author. Tel.: +81 43 226 2083; fax: +81 43 226 2088.

E-mail address: imazekif@faculty.chiba-u.jp (F. Imazeki).

Abbreviations: HCV, hepatitis C virus; IFN, interferon; HCC, hepatocellular carcinoma; SVR, sustained virological response; DW-type, double wild-type; RR, risk ratio; AST, aspartate aminotransferase; ALT, alanine aminotransferase; US, ultrasonography; CT, computed tomography; MRI, magnetic resonance imaging; PCR, polymerase chain reaction; OR, odds ratio.

Table 1. Baseline characteristics of 361 hepatitis C (HCV) genotype 1-infected patients according to hepatocellular carcinoma (HCC) development.

Patients	$n = 361$	HCC development		
		(+), $n = 82$	(−), $n = 279$	p value
Gender (male/female)	219/142	56/26	163/116	0.1
Age (years)	50.5 ± 12.2	56.8 ± 7.1	48.6 ± 12.7	<0.0001
BMI (kg/m^2)	23.1 ± 2.9	23.1 ± 2.8	23.1 ± 3.3	0.82
Staging of fibrosis (F0–1/F2/F3/F4)	197/59/52/53	13/18/23/28	184/41/29/25	<0.0001
IFN treatment and response				
SVR/non-SVR/non-IFN	73/202/86	4/55/23	69/147/63	0.0004
Laboratory data				
AST (IU/L)	87 ± 62	109 ± 59	80 ± 61	0.0001
ALT (IU/L)	125 ± 93	139 ± 80	121 ± 96	0.13
AST/ALT	0.75 ± 0.26	0.84 ± 0.28	0.73 ± 0.25	0.0003
Platelets (10^4/mm^3)	17.7 ± 6.7	13.0 ± 3.3	18.2 ± 6.9	<0.0001
Albumin (g/dL)	4.2 ± 0.36	4.1 ± 0.39	4.3 ± 0.35	<0.0001
Total bilirubin (mg/dL)	0.8 ± 0.6	0.9 ± 0.3	0.8 ± 0.6	0.39
Core protein (pg/mL)	201 ± 245	283 ± 273	177 ± 231	0.001
Amino acid pattern				
70 Wild/non-wild/ND	168/129/64	32/32/18	136/97/46	0.23*
91 Wild/non-wild/ND	139/158/64	28/36/18	111/122/46	0.58*
DW/non-DW/ND	81/216/64	12/52/18	69/164/46	0.08*

BMI, body mass index; DW, double wild (arginine at residue 70 and leucine at residue 91 in the core region); ND, not detected; ND cases were excluded.

The clinical backgrounds of the patients are shown in Table 1. The study population was predominantly male (59% men), and the mean age of the patients was 50.5 ± 12.2 years, with 15% patients having liver cirrhosis.

Laboratory examination

Serum samples were obtained and stored at −30 °C until analysis. We assumed that genotype 1 corresponds to group 1 when determining the HCV RNA genotypes by serologic grouping of serum antibodies [20]. The serum HCV load of the patients was determined at the time of liver biopsy, using the HCV core protein detection kit (Eiken Chemical, Tokyo, Japan; detection limit, 8 pg/mL) [21].

Histopathological examination

Percutaneous liver biopsy was performed, and specimens were histopathologically assessed as described previously [22]. According to the criteria of Desmet et al. [23], the staging of fibrosis was defined as F0 (no fibrosis), F1 (mild fibrosis), F2 (moderate fibrosis), F3 (severe fibrosis), and F4 (cirrhosis).

Core nucleotide sequences

HCV RNA was extracted from the serum samples obtained at the time of liver biopsy, and it was reverse-transcribed using SuperScript III reverse transcriptase (Invitrogen, Carlsbad, CA, USA). Nucleic acids were amplified by PCR with the

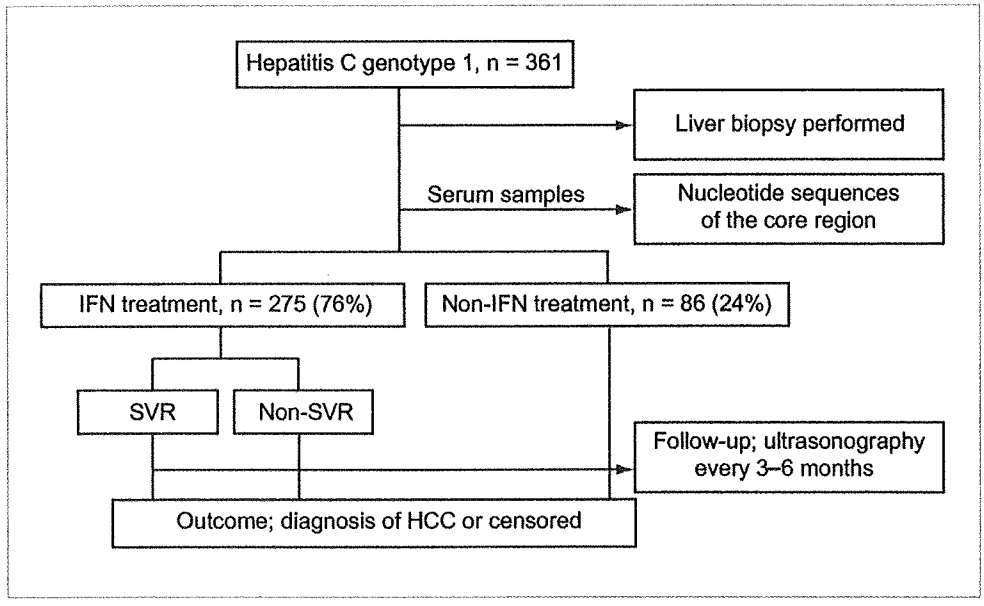

Fig. 1. Clinical courses after enrollment and the evaluation methods. IFN, interferon; SVR, sustained virological response; HCC, hepatocellular carcinoma. [This figure appears in colour on the web.]

HotStart Taq Master Mix kit (Qiagen, Hilden, Germany) and primers that have been previously described [24]. Polymerase chain reaction (PCR) was initiated with a denaturation step at 95 °C for 15 min, followed by 45 cycles at 94 °C for 1 min, 45 °C for 1 min, and 72 °C for 3 min, and subsequent extension for 7 min. PCR products were resolved by agarose gel electrophoresis, purified using the QIA quick PCR purification kit (Qiagen), and directly sequenced using a Big Dye Terminator v3.1 Cycle Sequencing kit (Applied Biosystems, Tokyo, Japan). The sequences were determined using an ABI PRISM 310 Genetic Analyzer (Applied Biosystems).

As described previously, the double wild-type (DW-type) amino acid pattern was defined as the presence of arginine at residue 70 (wild-type) and leucine at residue 91 (wild-type) [19].

IFN treatment

Depending on whether IFN was administered, the patients were divided into the IFN (76%) and non-IFN groups (24%) (Fig. 1). Patients who received IFN monotherapy during follow-up were divided into two subgroups: the sustained virological response (SVR) group, including patients who tested negative for HCV RNA at 24 weeks after completion of therapy, and non-SVR group (Fig. 1). Of the 275 patients in the IFN group, 73 (26.5%) achieved SVR.

Follow-up and diagnosis of cirrhosis and HCC

Clinical assessments were performed at least once every month during IFN treatment and every 3–6 months after the treatment. During follow-up, abdominal US was performed every 3–6 months to determine whether HCC had developed (Fig. 1). If necessary, additional procedures like CT, MRI, abdominal angiography, and US-guided tumor biopsy were performed to confirm HCC development. We also evaluated whether cirrhosis had developed in non-cirrhotic patients (F0–F2 stage). Cirrhosis was diagnosed according to the criteria of cirrhosis as described previously [25,26]. The follow-up period was the duration from the initial liver biopsy to HCC diagnosis or the last follow-up visit. For non-cirrhotic patients, this was the duration from the start point to cirrhosis diagnosis.

Statistical analysis

The χ^2 test was used to compare categorical variables, and Student's t test to compare continuous variables related to background characteristics among groups. Continuous variables were expressed as mean ± standard deviation. The cumulative incidence of HCC and cirrhosis was calculated using the Kaplan–Meier method and evaluated using the Breslow–Gehan–Wilcoxon test. Multivariate analysis was performed using the Cox proportional-hazards model or multiple logistic regression analysis. The Cochran–Armitage trend test was used for analyzing the association between the prevalence of mutation and subject age. Statistical significance was defined as $p < 0.05$.

Results

Cumulative HCC incidence

During follow-up (median duration, 121 months; range, 8–257 months), 82 (22.7%) patients developed HCC [HCC group; 13 of 197 (6.6%) from F0–F1, 18 of 59 (30.5%) from F2, 23 of 52 (44.2%) from F3, and 28 of 53 (52.8%) from F4 stage at entry] and 279 (77.3%) did not (non-HCC group). The cumulative HCC incidence at 5, 10, and 15 years of follow-up was 9.5%, 22.9%, and 30.9%, respectively.

Core nucleotide sequences

The core nucleotide sequence was determined for 297 of 361 (82.3%) patients. In the entire patient group, the proportions of DW-type and non-DW-type patterns were 22% and 60%, respectively (Table 1).

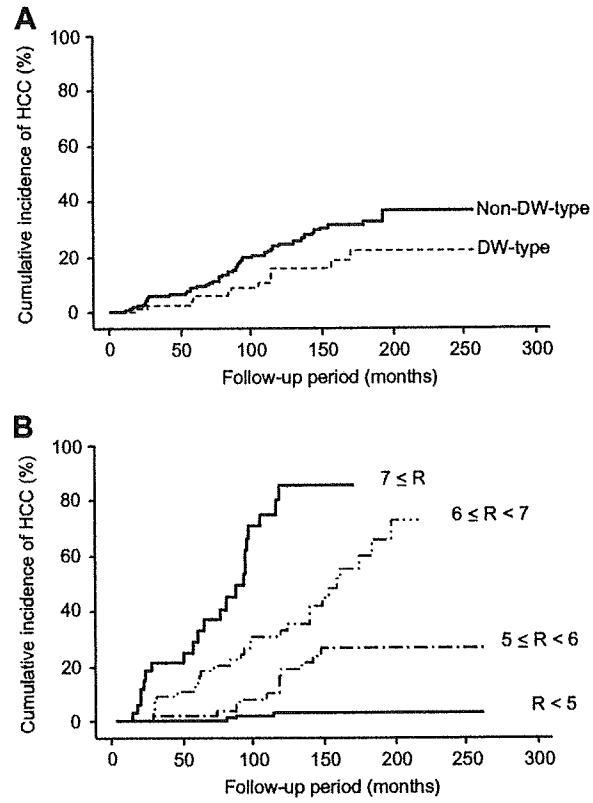

Fig. 2. Cumulative incidence of hepatocellular carcinoma (HCC) in hepatitis C genotype 1-infected patients. (A) Comparison between patients with double wild-type (DW-type: arginine, residue 70; leucine, residue 91) ($n = 81$) and non-DW-type ($n = 216$) amino acids in the core region ($p = 0.06$). (B) Comparison based on risk score (R) calculated using independent variables for HCC risk ($p < 0.0001$).

The core nucleotide sequence could not be determined for 64 patients because their samples showed significantly lower levels of the HCV core protein than those obtained from the 297 patients in whom the core sequence could be detected (119 vs. 217 pg/mL; $p = 0.0083$). There was no significant difference between the other variables shown in Table 1.

Cumulative HCC incidence according to core amino acid mutations

During follow-up, 12 of 81 (14.8%) patients with the DW-type pattern and 52 of 216 (24.1%) patients with the non-DW-type pattern developed HCC. Cumulative HCC incidence was 6.8% and 11% at 5 years, 19.1% and 27.7% at 10 years, and 26.6% and 38% at 15 years in the DW-type and non-DW-type groups, respectively. Cumulative HCC incidence in the DW-type group tended to be lower than that in the non-DW-type group ($p = 0.06$; Fig. 2A).

Predictive factors associated with HCC development

Potential predictive factors associated with HCC development are shown in Table 1. Univariate analysis revealed 10 parameters correlating with HCC development (Table 1). Multivariate analy-

Table 2. Factors associated with hepatocellular carcinoma development in hepatitis C genotype 1-infected patients, identified by multivariate analysis using the Cox proportional-hazards model.

Factor*	Category	Risk ratio (95% CI)	p value
Gender	Male	3.97 (2.05–7.63)	<0.0001
	Female	1.0	
Age (years)	⩾50	2.08 (1.01–4.33)	0.049
	<50	1.0	
Staging of fibrosis	⩾2	5.75 (2.68–12.35)	<0.0001
	<2	1.0	
IFN treatment and response	Absence of SVR	10.0 (2.29–43.48)	0.002
	SVR	1.0	
AST (IU/L)	>90	2.08 (1.20–3.62)	0.009
	⩽90	1.0	
AST/ALT	⩾0.8	2.21 (1.24–3.97)	0.007
	<0.8	1.0	
Amino acid pattern	Non-DW	1.96 (1.02–3.76)	0.04
	DW	1.0	

CI, confidence intervals; DW, double wild (arginine at residue 70 and leucine at residue 91 in the core region).
*Significant factors are shown.

sis with the Cox proportional-hazards model showed that the following seven independent parameters were significantly associated with HCC development: male gender ($p < 0.0001$), age ⩾ 50 years ($p = 0.049$), fibrosis ⩾ F2 ($p < 0.0001$), absence of SVR ($p = 0.002$), aspartate aminotransferase (AST) level > 90 IU/L ($p = 0.009$), AST/alanine aminotransferase (ALT) ratio ⩾ 0.8 ($p < 0.007$), and non-DW-type pattern in the core region ($p = 0.04$) (Table 2).

Prediction of HCC development based on risk score

Using the predictive variables from the previous step (Table 2), the risk score (R) for HCC development was calculated from the beta coefficients derived from the Cox proportional-hazards model as follows: $R = 0.671 \times$ (non-DW-type) + $2.307 \times$ (absence of SVR) + $0.733 \times$ (AST > 90 IU/L) + $0.733 \times$ (age ⩾ 50 years) + $1.752 \times$ (staging of fibrosis ⩾ 2) + $1.378 \times$ (male) + $0.795 \times$ (AST/ALT ⩾ 0.8) (each variable: yes = 1, no = 0). Fig. 2B shows the cumulative HCC incidence of four subgroups categorized by risk score, and the RR of each group is shown in Table 3. The cumulative HCC incidence increased with the risk score: from highest to lowest it was 84.7%, 35.1%, 18.5%, and 3.0% at 10 years.

Cumulative HCC incidence according to IFN treatment and response

During follow-up, 4 (5.5%) patients in the SVR, 55 (27.2%) in the non-SVR, and 23 (26.7%) in the non-IFN groups developed HCC; cumulative HCC incidence was 0%, 11.3%, and 13.2%, respectively, at 5 years; 7.8%, 25.6%, and 27.3%, respectively, at 10 years; and 7.8%, 36.5%, and 35.5%, respectively, at 15 years. Moreover, cumulative HCC incidence was significantly lower in the SVR group than other groups ($p < 0.001$; Fig. 3).

Table 3. Relative risk of HCC development based on risk score, using the Cox proportional-hazards model.

Score (R)	Risk ratio (95% CI)	p value
$R < 5$	1	
$5 \leqslant R < 6$	9.22 (2.60–32.7)	0.0006
$6 \leqslant R < 7$	26.9 (8.15–89.0)	<0.0001
$7 \leqslant R$	88.3 (25.8–302)	<0.0001

CI, confidence intervals.

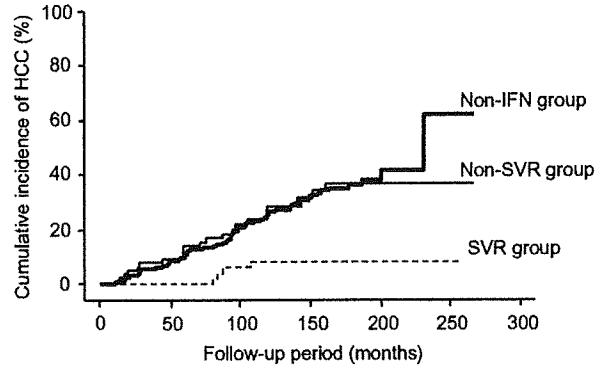

Fig. 3. Cumulative incidence of hepatocellular carcinoma (HCC). Comparison between the sustained virological response (SVR) ($n = 73$), non-SVR ($n = 202$), and non-interferon (IFN) ($n = 86$) groups ($p = 0.002$).

Analysis of SVR-associated factors

Compared to those in the non-IFN group, patients in the IFN group were younger (49 years vs. 54 years, $p = 0.003$), had higher aminotransferase levels (AST, 93 vs. 68 IU/L, $p = 0.001$; ALT, 137 vs. 87 IU/L, $p < 0.0001$) and lower core protein levels (183 vs. 263 pg/mL, $p = 0.01$). Table 4 shows baseline characteristics of patients according to interferon response. Univariate analysis revealed six SVR-associated parameters, whereas multiple logistic regression analysis revealed two independent significant predictors of SVR: AST/ALT ratio of <0.8 [$p = 0.005$; odds ratio (OR), 3.09; 95% confidence interval (CI), 1.40–6.82] and core protein level of <200 pg/mL [$p < 0.0001$; OR, 70.94; 95% CI, 9.56–526.2]. However, both univariate ($p = 0.64$) and multivariate analyses (data not shown) showed that the DW-type pattern in the core region was not associated with SVR.

Table 4. Baseline characteristics of patients according to interferon response.

Nature of the Regime	SVR $n = 73$	Non-SVR $n = 202$	p value
Gender (Male/Female)	47/26	126/76	0.76
Age (years)	46.6 ± 13.3	50.5 ± 11.5	0.02
BMI (kg/m^2)	22.7 ± 2.8	23.2 ± 3.0	0.24
Staging of fibrosis: (F0-1/F2/F3/F4)	45/12/9/7	104/34/34/30	0.42
Laboratory data			
AST (IU/L)	79 ± 56	97 ± 69	0.048
ALT (IU/L)	132 ± 92	139±100	0.60
AST/ALT	0.65 ± 0.22	0.75 ± 0.27	0.003
Platelets (10^4/mm^3)	18.6 ± 6.7	16.7 ± 6.1	0.03
Albumin (g/dL)	4.3 ± 0.3	4.2 ± 0.4	0.06
Total bilirubin (mg/dL)	0.7 ± 0.4	0.8 ± 0.4	0.02
Core protein (pg/mL)	31 ± 50	234 ± 226	<0.0001
Amino acid pattern			
70 Wild/Non-wild/ND	35/21/17	89/74/39	0.30
91 Wild/Non-wild/ND	24/32/17	76/87/39	0.62
DW/Non-DW/ND	14/42/17	46/117/39	0.64

BMI, body mass index; DW, double wild (arginine at residue 70 and leucine at residue 91 in the core region); ND, not detected.

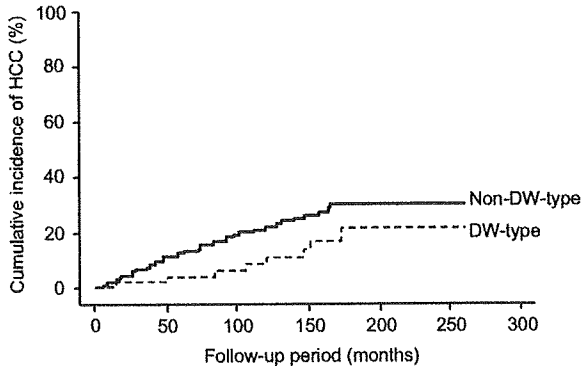

Fig. 4. Cumulative incidence of cirrhosis in non-cirrhotic patients (F0–F2). Comparison between patients with double wild-type (DW-type: arginine, residue 70; leucine, residue 91) ($n = 81$) and non-DW-type ($n = 216$) amino acids in the core region ($p = 0.051$).

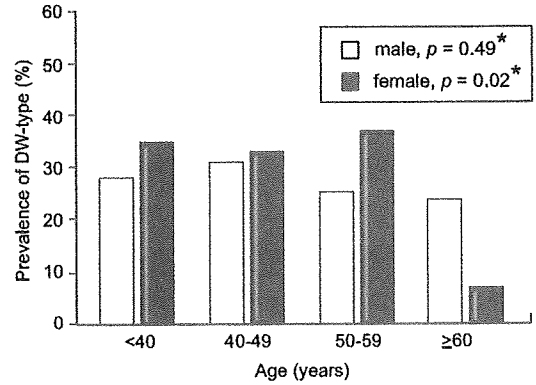

Fig. 5. Prevalence of double wild-type (DW-type: arginine, residue 70; leucine, residue 91) amino acids in the hepatitis C core region according to age and gender. *By the Cochran-Armitage trend test.

Cumulative cirrhosis incidence for non-cirrhotic patients (F0–F2)

Of the 256 non-cirrhotic patients (197 from F0–F1, 59 from F2), 50 (19.5%) developed cirrhosis (cirrhosis group) and 206 (80.5%) did not (non-cirrhosis group). The cumulative cirrhosis incidence at 5, 10, and 15 years of follow-up was 9.7%, 18.2%, and 26.4%, respectively. The HCC incidence was higher in the cirrhosis group [23/50 (46%)] than the non-cirrhosis group [8/206 (3.9%); $p < 0.0001$]. In the entire population, 71 of 82 (86.6%) patients who developed HCC had underlying cirrhosis and 11 (13.4%) did not, when HCC was detected ($p < 0.0001$).

Cumulative cirrhosis incidence according to the amino acid pattern in the core region for F0–F2 patients

The cumulative cirrhosis incidence tended to be higher in the non-DW-type group than the DW-type group (11.9% and 3.6% at 5 years, 21.5% and 10.4% at 10 years, and 29.7% and 20.7% at 15 years of follow-up, respectively; $p = 0.051$; Fig. 4).

Analysis of factors associated with cirrhosis development in F0–F2 patients

We analyzed the factors associated with cirrhosis development in patients with F0–F2 fibrosis at enrollment. Univariate analysis revealed nine parameters correlating with cirrhosis development: male gender ($p = 0.04$), older age ($p < 0.0001$), advanced fibrosis ($p < 0.0001$), absence of SVR ($p < 0.0001$), high AST level ($p < 0.0001$), high ALT level ($p = 0.01$), high AST/ALT ratio ($p = 0.001$), low platelet count ($p = 0.0009$), and high core protein level ($p = 0.02$). Multivariate analysis, including analysis of the amino acid pattern in the core region with the Cox proportional-hazards model, showed that the following three independent parameters were significantly associated with cirrhosis development: male gender ($p = 0.004$), fibrosis = F2 ($p = 0.004$), and absence of SVR ($p = 0.02$). Meanwhile, the presence of the non-DW-type pattern in the core region tended to lead to cirrhosis development (RR, 2.13; 95% CI, 0.93–4.91; $p = 0.07$).

Analysis of factors associated with mutations at core residues 70 and 91

Eighty-one patients with the DW-type pattern at core residues 70 and 91, who were at low risk for HCC, tended to be younger than the 216 patients with the non-DW-type pattern, who were at high risk for HCC (48.4 ± 11.8 years vs. 51.1 ± 11.8 years, respectively; $p = 0.08$). Separate analysis of men and women (Fig. 5) showed that the DW-type pattern was rare in women aged 60 years or above ($p = 0.02$).

Consistent with these results, HCC incidence was the same in men and women aged 60 or above (19% vs. 10% at 5 years and 32% vs. 38% at 10 years of follow-up, respectively; $p = 0.89$); however, in patients aged less than 60 years, HCC incidence was lower in women than in men (4% vs. 11% at 5 years and 15% vs. 22% at 10 years of follow-up, respectively; $p = 0.03$).

Discussion

Male gender, older age, advanced-stage fibrosis, and no IFN treatment are reported as important predictors of HCC development in chronic hepatitis C patients [4–7]. Viral factors associated with HCC development were also reported [27–29]. Several studies showed that mutations in the core protein are associated with HCC among HCV genotype 1b-infected patients, but the results varied between studies [18,30,31]. Consistent with a report by Akuta et al. [18], we showed that the presence of the non-DW-type pattern at core residues 70 and 91 is an independent risk factor for HCC development. Akuta et al. [18] studied 313 chronic hepatitis C patients who received IFN therapy (101 were excluded), and found that non-DW-type was an independent risk factor for HCC development (RR, 5.92; 95% CI, 1.58–22.2; $p = 0.008$) by using the Cox proportional-hazards model, and its correlation with HCC risk was stronger than that found in our study (RR, 1.96; 95% CI, 1.02–3.76; $p = 0.04$). We analyzed cirrhotic patients (14.7% of total population), most of whom developed HCC, and also non-cirrhotic patients, and found that the non-DW-type was still an independent risk factor for HCC development (RR, 2.90; 95% CI, 1.11–7.61; $p = 0.03$). Furthermore, we

found that the non-DW-type in patients with F0–F2 fibrosis was likely to lead to cirrhosis, diagnosed by US ($p = 0.051$). Moreover, the non-DW-type in patients with F0–F3 fibrosis was significantly associated with cirrhosis development ($p = 0.007$, data not shown). These results suggest that the non-DW-type may affect HCC development by accelerating cirrhosis development; however, prospective studies of histological findings are needed to confirm this.

It is unclear why the amino acids at residues 70 and 91 affect HCC development. The core protein cooperates with the Ras oncogene and transforms primary rat embryo fibroblasts into the tumorigenic phenotype [10]. The HCV core protein (residues 25–91) also interacts with the heterogeneous nuclear ribonucleoprotein K, which stimulates the c-myc promoter, downstream of the Wnt/beta-catenin signal [11]. Pavio et al. reported that the HCV core (residues 59–126, residues at 70 and 91 were non-wild-type) interacts with Smad3 and inhibits the TGF-beta pathway, important in apoptosis [12]. Mutations in the clustering variable regions (residues 39–76) are often seen in HCC patients [30], and mutations in the *N*-myristoylation sites (e.g., residue 91) in the core region, are associated with growth control and virus replication [31]. Delhem et al. have shown that the core protein with non-wild-type amino acids at residues 70 and 91 obtained from a HCC patient binds and activates PKR, which might cause carcinogenesis [13]. It was reported that the presence of a non-wild-type amino acid at residue 91 enhances internal initiation of HCV protein synthesis, leading to the expression of a core isoform, which may interact with viral and cellular components [32]. These results suggest that residues 70 and 91 themselves or via interactions with adjacent amino acids may be involved in HCC development; however, further studies are needed to evaluate the effect of core mutations on HCC development.

The presence of the DW-type pattern in the core region is also reportedly a predictor of the virological response to therapy with peginterferon and ribavirin [19]. With this therapy, an SVR of approximately 50% could be achieved by HCV genotype 1-infected patients having high viral load. We found the absence of an SVR and the non-DW-type pattern to be predictors of HCC development; however, the non-DW-type pattern was not a predictor of the absence of an SVR. This may be partly because we used IFN monotherapy without ribavirin, with which the SVR rate (26.5% in our study) was lower than that with peginterferon plus ribavirin [33,34]. Therefore, we believe that combination therapy, rather than IFN monotherapy, would more efficiently eradicate HCV with the DW-type pattern in the core region; however, further studies are required to test this hypothesis. Our current focus is on a prospective study to examine the association between core mutations and the outcome of combination treatment with peginterferon plus ribavirin.

Our study revealed that the DW-type pattern, associated with a low HCC risk, was rare in women aged 60 years or above. This may explain why HCC incidence in women was as high as that in men. The underlying mechanisms by which age or gender influence core-region mutations are unknown. In previous studies, a mutation at residue 70 was correlated with virological response to therapy with IFN plus ribavirin [17] and with AFP levels [35] in HCV genotype 1b-infected patients without HCC. Further follow-up studies must examine whether a mutation occurs in the wild-type amino acid.

We investigated two specific amino acid mutations in the HCV core region by direct sequencing. The HCV core sequence can be easily amplified using PCR because of its conservative nature and analysis of only two amino acid positions is timesaving; therefore, this method might be feasible for identifying predictive markers for HCC. A specific PCR method for detecting these mutations was reported [36]. Furthermore, we developed a rapid and sensitive real-time PCR method for quantitatively detecting these mutations [37]. We hope this method can be used to detect HCV sequences in case of a low viral load, and believe that it will be more useful for predicting HCC.

In conclusion, HCC risk could be predicted by studying mutations in the HCV core region, response to IFN, and host factors like age, gender, and liver fibrosis in HCV genotype 1-infected patients. These mutations might be involved in an oncogenic mechanism leading to HCC development in chronic HCV patients.

Financial disclosures

All authors have nothing to disclose.

Acknowledgements

The authors who have taken part in this study declared that they do not have anything to disclose regarding funding from industries or conflict of interest with respect to this manuscript.

References

[1] Seeff LB. Natural history of chronic hepatitis C. Hepatology 2002;36:S35–S46.
[2] Saito I, Miyamura T, Ohbayashi A, Harada H, Katayama T, Kikuchi S, et al. Hepatitis C virus infection is associated with the development of hepatocellular carcinoma. Proc Natl Acad Sci USA 1990;87:6547–6549.
[3] Poynard T, Bedossa P, Opolon P. Natural history of liver fibrosis progression in patients with chronic hepatitis C. The OBSVIRC, METAVIR, CLINIVIR, and DOSVIRC groups. Lancet 1997;349:825–832.
[4] Yoshida H, Shiratori Y, Moriyama M, Arakawa Y, Ide T, Sata M, et al. Interferon therapy reduces the risk for hepatocellular carcinoma: national surveillance program of cirrhotic and noncirrhotic patients with chronic hepatitis C in Japan. IHIT Study group. Inhibition of hepatocarcinogenesis by interferon therapy. Ann Intern Med 1999;131:174–181.
[5] Freeman AJ, Dore GJ, Law MG, Thorpe M, Von Overbeck J, Lloyd AR, et al. Estimating progression to cirrhosis in chronic hepatitis C virus infection. Hepatology 2001;34:809–816.
[6] Fartoux L, Chazouilleres O, Wendum D, Poupon R, Serfaty L. Impact of steatosis on progression of fibrosis in patients with mild hepatitis C. Hepatology 2005;41:82–87.
[7] Lok AS, Seeff LB, Morgan TR, di Bisceglie AM, Sterling RK, Curto TM, et al. Incidence of hepatocellular carcinoma and associated risk factors in hepatitis C-related advanced liver disease. Gastroenterology 2009;136:138–148.
[8] Simmonds P, Bukh J, Combet C, Deleage G, Enomoto N, Feinstone S, et al. Consensus proposals for a unified system of nomenclature of hepatitis C virus genotypes. Hepatology 2005;42:962–973.
[9] Ikeda K, Kobayashi M, Someya T, Saitoh S, Tsubota A, Akuta N, et al. Influence of hepatitis C virus subtype on hepatocellular carcinogenesis: a multivariate analysis of a retrospective cohort of 593 patients with cirrhosis. Intervirology 2002;45:71–78.
[10] Ray RB, Lagging LM, Meyer K, Ray R. Hepatitis C virus core protein cooperates with ras and transforms primary rat embryo fibroblasts to tumorigenic phenotype. J Virol 1996;70:4438–4443.
[11] Hsieh TY, Matsumoto M, Chou HC, Schneider R, Hwang SB, Lee AS, et al. Hepatitis C virus core protein interacts with heterogeneous nuclear ribonucleoprotein K. J Biol Chem 1998;273:17651–17659.
[12] Pavio N, Battaglia S, Boucreux D, Arnulf B, Sobesky R, Hermine O, et al. Hepatitis C virus core variants isolated from liver tumor but not from

adjacent non-tumor tissue interact with Smad3 and inhibit the TGF-beta pathway. Oncogene 2005;24:6119–6132.
[13] Delhem N, Sabile A, Gajardo R, Podevin P, Abadie A, Blaton MA, et al. Activation of the interferon-inducible protein kinase PKR by hepatocellular carcinoma derived-hepatitis C virus core protein. Oncogene 2001;20:5836–5845.
[14] Moriya K, Fujie H, Shintani Y, Yotsuyanagi H, Tsutsumi T, Ishibashi K, et al. The core protein of hepatitis C virus induces hepatocellular carcinoma in transgenic mice. Nat Med 1998;4:1065–1067.
[15] Perlemuter G, Sabile A, Letteron P, Vona G, Topilco A, Chretien Y, et al. Hepatitis C virus core protein inhibits microsomal triglyceride transfer protein activity and very low density lipoprotein secretion: a model of viral-related steatosis. FASEB J 2002;16:185–194.
[16] Honda A, Hatano M, Kohara M, Arai Y, Hartatik T, Moriyama T, et al. HCV-core protein accelerates recovery from the insensitivity of liver cells to Fas-mediated apoptosis induced by an injection of anti-Fas antibody in mice. J Hepatol 2000;33:440–447.
[17] Donlin MJ, Cannon NA, Yao E, Li J, Wahed A, Taylor MW, et al. Pretreatment sequence diversity differences in the full-length hepatitis C virus open reading frame correlate with early response to therapy. J Virol 2007;81:8211–8224.
[18] Akuta N, Suzuki F, Kawamura Y, Yatsuji H, Sezaki H, Suzuki Y, et al. Amino acid substitutions in the hepatitis C virus core region are the important predictor of hepatocarcinogenesis. Hepatology 2007;46:1357–1364.
[19] Akuta N, Suzuki F, Kawamura Y, Yatsuji H, Sezaki H, Suzuki Y, et al. Predictive factors of early and sustained responses to peginterferon plus ribavirin combination therapy in Japanese patients infected with hepatitis C virus genotype 1b: amino acid substitutions in the core region and low-density lipoprotein cholesterol levels. J Hepatol 2007;46: 403–410.
[20] Tanaka T, Tsukiyama-Kohara K, Yamaguchi K, Yagi S, Tanaka S, Hasegawa A, et al. Significance of specific antibody assay for genotyping of hepatitis C virus. Hepatology 1994;19:1347–1353.
[21] Tanaka E, Kiyosawa K, Matsumoto A, Kashiwakuma T, Hasegawa A, Mori H, et al. Serum levels of hepatitis C virus core protein in patients with chronic hepatitis C treated with interferon alfa. Hepatology 1996;23:1330–1333.
[22] Imazeki F, Yokosuka O, Fukai K, Saisho H. Favorable prognosis of chronic hepatitis C after interferon therapy by long-term cohort study. Hepatology 2003;38:493–502.
[23] Desmet VJ, Gerber M, Hoofnagle JH, Manns M, Scheuer PJ. Classification of chronic hepatitis: diagnosis, grading and staging. Hepatology 1994;19:1513–1520.
[24] Enomoto N, Sakuma I, Asahina Y, Kurosaki M, Murakami T, Yamamoto C, et al. Comparison of full-length sequences of interferon-sensitive and resistant hepatitis C virus 1b. Sensitivity to interferon is conferred by amino acid substitutions in the NS5A region. J Clin Invest 1995;96:224–230.
[25] Simonovsky V. The diagnosis of cirrhosis by high resolution ultrasound of the liver surface. Br J Radiol 1999;72:29–34.
[26] Kudo M, Zheng RQ, Kim SR, Okabe Y, Osaki Y, Iijima H, et al. Diagnostic accuracy of imaging for liver cirrhosis compared to histologically proven liver cirrhosis. A multicenter collaborative study. Intervirology 2008;51:17–26.
[27] Ogat S, Ku Y, Yoon S, Makino S, Nagano-Fujii M, Hotta H. Correlation between secondary structure of an amino-terminal portion of the nonstructural protein 3 (NS3) of hepatitis C virus and development of hepatocellular carcinoma. Microbiol Immunol 2002;46:549–554.
[28] Gimenez-Barcons M, Franco S, Suarez Y, Forns X, Ampurdanes S, Puig-Basagoiti F, et al. High amino acid variability within the NS5A of hepatitis C virus (HCV) is associated with hepatocellular carcinoma in patients with HCV-1b-related cirrhosis. Hepatology 2001;34:158–167.
[29] De Mitri MS, Morsica G, Cassini R, Bagaglio S, Zoli M, Alberti A, et al. Prevalence of wild-type in NS5A-PKR protein kinase binding domain in HCV-related hepatocellular carcinoma. J Hepatol 2002;36:116–122.
[30] Shimizu I, Yao DF, Horie C, Yasuda M, Shiba M, Horie T, et al. Mutations in a hydrophilic part of the core gene of hepatitis C virus in patients with hepatocellular carcinoma in China. J Gastroenterol 1997;32:47–55.
[31] Horie T, Shimizu I, Horie C, Yogita S, Tashiro S, Ito S. Mutations of the core gene sequence of hepatitis C virus isolated from liver tissues with hepatocellular carcinoma. Hepatol Res 1999;13:240–251.
[32] Eng FJ, Walewski JL, Klepper AL, Fishman SL, Desai SM, McMullan LK, et al. Internal initiation stimulates production of p8 minicore, a member of a newly discovered family of hepatitis C virus core protein isoforms. J Virol 2009;83:3104–3114.
[33] Schalm SW, Hansen BE, Chemello L, Bellobuono A, Brouwer JT, Weiland O, et al. Ribavirin enhances the efficacy but not the adverse effects of interferon in chronic hepatitis C. Meta-analysis of individual patient data from European centers. J Hepatol 1997;26:961–966.
[34] Mangi A, Villani MR, Minerva N, Leandro G, Bacca D, Cela M, et al. Efficacy of 5 MU of interferon in combination with ribavirin for naive patients with chronic hepatitis C virus: a randomized controlled trial. J Hepatol 2001;34:441–446.
[35] Akuta N, Suzuki F, Kawamura Y, Yatsuji H, Sezaki H, Suzuki Y, et al. Substitution of amino acid 70 in the hepatitis C virus core region of genotype 1b is an important predictor of elevated alpha-fetoprotein in patients without hepatocellular carcinoma. J Med Virol 2008;80:1354–1362.
[36] Okamoto K, Akuta N, Kumada H, Kobayashi M, Matsuo Y, Tazawa H. A nucleotide sequence variation detection system for the core region of hepatitis C virus-1b. J Virol Methods 2007;141:1–6.
[37] Nakamoto S, Kanda T, Yonemitsu Y, Arai M, Fujiwara K, Fukai K, et al. Quantification of hepatitis C amino acid substitutions 70 and 91 in the core coding region by real-time amplification refractory mutation system reverse transcription-polymerase chain reaction. Scand J Gastroenterol 2009:1–6.

G Model
EURR-4527; No. of Pages 5
ARTICLE IN PRESS

European Journal of Radiology xxx (2009) xxx–xxx

Contents lists available at ScienceDirect

European Journal of Radiology

journal homepage: www.elsevier.com/locate/ejrad

Changes in tumor vascularity precede microbubble contrast accumulation deficit in the process of dedifferentiation of hepatocellular carcinoma

Hitoshi Maruyama*, Masanori Takahashi, Hiroyuki Ishibashi, Shinichiro Okabe, Masaharu Yoshikawa, Osamu Yokosuka

Department of Medicine and Clinical Oncology, Chiba University Graduate School of Medicine 1-8-1, Inohana, Chuou-ku, Chiba 260-8670, Japan

ARTICLE INFO

Article history:
Received 19 June 2009
Received in revised form 22 August 2009
Accepted 25 August 2009

Keywords:
Ultrasound
Hepatocellular carcinoma
Contrast agent
Sonazoid
Nodule-in-nodule

ABSTRACT

Purpose: To elucidate the changes in tumor vascularity and microbubble accumulation on contrast-enhanced sonograms, in relation to the dedifferentiation of hepatocellular carcinoma (HCC).
Materials and methods: This prospective study enrolled 10 patients with histologically proven HCC (14.4–39.0 mm, 26.1 ± 7.4) showing nodule-in-nodule appearance upon contrast-enhanced computed tomography. Contrast-enhanced ultrasound was performed by harmonic imaging under a low mechanical index (0.22–0.25) during the vascular phase (agent injection to 1 min) and late phase (15 min) following the injection of Sonazoid™ (0.0075 ml/kg). Contrast enhancement in the inner and outer nodules was assessed in comparison with that in adjacent liver parenchyma as hyper-, iso-, or hypo-enhanced.
Results: Vascular-phase enhancement of all 10 inner nodules was hyper-enhanced, and that of outer nodules was hyper-enhanced in 3, iso-enhanced in 2, and hypo-enhanced in 5. Late-phase enhancement of inner nodules was hypo-enhanced in 8 and iso-enhanced in 2. Furthermore, late-phase enhancement of outer nodules was iso-enhanced in the 7 lesions that showed iso- or hypo-enhancement in the vascular phase, and hypo-enhanced in the 3 with hyper-enhancement in the vascular phase. Late-phase hypo-enhancement was significantly more frequent in the nodules showing early-phase hyper-enhancement (11/13) than in the nodules showing early-phase iso- or hypo-enhancement (0/7) in both the inner and outer nodules.
Conclusion: Dedifferentiation of HCC may be accompanied by changes in tumor vascularity prior to a reduction in microbubble accumulation. Observation of the vascular phase may be more useful than late-phase imaging for the early recognition of HCC dedifferentiation when using contrast-enhanced ultrasound with Sonazoid.

1. Introduction

Hepatocellular carcinoma (HCC) is one of the most common malignancies, and its incidence is increasing worldwide, especially in the eastern part of Asia [1,2]. The diagnosis of HCC is an issue of critical importance, in part because the prognosis of patients with cirrhosis depends to a large extent on the occurrence and progression of this neoplasm. Considering the limitations of tumor markers such as alpha fetoprotein (AFP) for HCC surveillance, it is necessary to have easy access to imaging examinations for cirrhotic patients [3,4].

Intra-tumor vascularity changes during the multistep process of carcinogenesis in HCC, including the presence of numerous tumor vessels, as well as a paucity of Kupffer cells comprise the well-known pathological appearance that is characteristic of HCC [5–7]. However, some well-differentiated HCCs have a hypo- or iso-vascular appearance, along with Kupffer cells distributed within the tumor nodule [6,7]. The relationship between the changes in tumor vascularity and Kupffer cell distribution, in accordance with the dedifferentiation process of HCC, has not been fully addressed in previous studies.

Contrast-enhanced ultrasound (US) has become popular as a non-invasive diagnostic tool for assessing focal hepatic lesions, due to the recent advances in digital technology incorporated into US equipment [8–10]. Microbubble contrast agents can be divided into two classes based on whether they do or do not accumulate in the liver, and both Levovist® (Schering, Berlin, Germany) and Sonazoid™ (GE Healthcare, Oslo, Norway) are classified as the former. They provide images of static microbubbles, which appear to demonstrate the function of the reticuloendothelial system such as phagocytosis by Kupffer cells, as well as imaging dynamic microbubbles that depict the hemodynamic circulation [11–14]. Therefore, contrast-enhanced US with these microbubble

* Corresponding author. Tel.: +81 43 2262083; fax: +81 43 2262088.
E-mail addresses: maru-cib@umin.ac.jp (H. Maruyama), machat@aa.pial.jp (M. Takahashi), bashiish@yahoo.co.jp (H. Ishibashi), okabeshin1966@yahoo.co.jp (S. Okabe), yoshikawa@faculty.chiba-u.jp (M. Yoshikawa), yokosukao@faculty.chiba-u.jp (O. Yokosuka).

0720-048X/$ – see front matter © 2009 Elsevier Ireland Ltd. All rights reserved.
doi:10.1016/j.ejrad.2009.08.017

contrast agents may reveal both tumor vascularity and Kupffer cell distribution in HCC lesions.

The nodule-in-nodule appearance of HCCs is a pattern that reflects cell dedifferentiation, because tumor elements with varying degrees of differentiation coexist in a single mass [15–20]. Assessment of contrast-enhanced US findings in HCCs with nodule-in-nodule appearance may reveal the dedifferentiation-related changes involved with tumor neovascularity and Kupffer cell distribution in these HCC lesions [21]. Against this background, we examined differences in contrast enhancement between the inner and outer nodules in HCC lesions having a nodule-in-nodule appearance. The purpose of this study was to elucidate the changes in tumor vascularity and microbubble accumulation exhibited on contrast-enhanced sonograms, in relation to the dedifferentiation of HCC.

2. Patients and methods

2.1. Patients

During the period from July 2007 to February 2009, a prospective study approved by the Ethics Committee of Chiba University Hospital, Chiba, Japan, was performed to examine Sonazoid-induced enhancement on sonograms of patients with HCC, after obtaining their informed written consent. A total of 513 patients with HCC underwent both contrast-enhanced computed tomography (CT) and contrast-enhanced US examination during this time period. There were 10 consecutive patients with HCC showing a nodule-in-nodule appearance upon contrast-enhanced CT, specifically, an inner nodule with hypervascularity and an outer nodule with a hypo-, iso-, or slightly hypervascular appearance on the images in the hepatic artery-dominant phase. The study enrolled these 10 cirrhotic patients as subjects, with all their HCC lesions proven histologically. The study patients consisted of 5 males and 5 females, with a mean age ± standard deviation (SD) of 67.3 ± 8.9 years (range 45–78 years). The diagnosis of liver cirrhosis was based on imaging findings, along with clinical symptoms and biochemistry results in all 10 patients; 9 of the patients were positive for hepatitis C virus antibody, and one patient was positive for hepatitis B virus surface antigen.

Each patient had one HCC tumor mass with a nodule-in-nodule appearance and a maximum diameter ranging from 14.4 to 39.0 mm (mean 26.1 ± 7.4 mm) on the sonogram. The serum AFP level ranged from 3.4 to 1266.1 ng/ml, with normal values (<20 ng/ml) found in 6 patients and abnormal values in 4 patients. No patients had egg allergy, which is a contraindication to the use of Sonazoid.

2.2. US examination

US examination was performed using the SSA-790A system (Aplio XG; Toshiba Medical Systems, Tokyo, Japan) with a 3.75-MHz convex probe. All patients underwent US examination after a fast of more than 4 h. At first, non-contrast grey-scale US (tissue harmonic imaging, 2.5/5.0 MHz, 14–27 Hz) was performed to observe the tumor appearance, to measure the diameters of the inner and outer nodules, and to select the scan plane allowing the most stable observation for contrast-enhanced US. Subsequently, color Doppler US was used to check for the presence or absence of vascular abnormality, such as arterio-portal communication, portal vein thrombosis, and/or portal vein tumor thrombosis. Next, the settings of the US system were changed for contrast-enhanced US, that is, to use the pulse subtraction harmonic imaging mode with a mechanical index level from 0.22 to 0.25, which is a low level in accordance with our previous report [22]. Gain was adjusted to an optimal level, and the dynamic range was set at 45–50 dB.

The contrast agent Sonazoid (perflubutane microbubbles with a median diameter of 2–3 μm) was used at a dose of 0.0075 ml/kg administered by manual bolus injection, followed by 3.0 ml of normal saline (administered by H.I.). Contrast enhancement was observed during two phases: the vascular phase (from contrast agent injection to 1 min, which is the early phase) and late phase (15 min after injection), under breath-holding as often as possible. For all patients, the operator performing the US examinations was M.T. (who had 7 years of experience in US examination). All US images recorded digitally were reviewed using frame-by-frame playback at a later date by H.M. (who had 19 years of experience in US examination), and contrast enhancement in the inner and outer nodules of the HCC lesions was assessed in comparison with that in adjacent liver parenchyma as hyper-, iso-, or hypo-enhanced in appearance.

2.3. Contrast-enhanced CT

Contrast-enhanced CT with dynamic imaging was performed in all patients using the Lightspeed Ultra16 (GE Yokogawa Medical Systems, Hino, Japan) with injection of 100 ml of contrast medium (Iopamiron 350; Nihon Schering, Osaka, Japan) at 3 ml/s into the antecubital vein by means of a mechanical injection system (Mark V ProVis, MEDRAD, Warrendale, PA, USA). Imaging was performed with a 30-s delay between contrast medium administration and start of imaging for the hepatic artery-dominant phase, 80-s delay for the portal vein-dominant phase, and 180-s delay for the equilibrium phase. The contrast-enhanced CT findings were evaluated by M.Y., who had 28 years of experience in heaptology, and was blinded to the patient information.

2.4. Pathological examination of HCC lesions

Pathological examination was performed on specimens obtained from 9 HCC lesions by percutaneous US-guided needle biopsy using a Sonopsy C1 needle (Hakko, Tokyo, Japan). Separate sampling from the inner and outer nodules was performed for 2 HCC lesions, although only a single sample was taken from the other 7 HCC lesions due to technical difficulties. All needle biopsies were performed by S.O. after US examination, and the time lag between contrast-enhanced US examination and needle biopsy ranged from 1 to 14 days (mean 4.5 ± 4.1 days). Pathological results were obtained from the surgically resected specimen in the case of one HCC lesion, with the time lag between contrast-enhanced US examination and surgical treatment being 2 months.

2.5. Statistical analysis

All data were expressed as means ± SD or percentages. Statistical significance was analyzed by using the Chi-square test, and p-values <0.05 were considered to be significant. Statistical analysis was performed using the SPSS software package (Version 13.0J; SPSS Inc., Chicago, IL, USA).

3. Results

3.1. Non-contrast US findings in HCC

Grey-scale US showed 5 lesions with a hyperechoic outer nodule and hypoechoic inner nodule, 2 lesions with a hypoechoic outer nodule and isoechoic inner nodule, one lesion with an isoechoic outer nodule and hypoechoic inner nodule, and one lesion with a hypoechoic outer nodule and hyperechoic inner nodule. In these 9 lesions, grey-scale US could clearly discriminate the outer nodule from the inner nodule, and the diameter of the inner nodules ranged from 6.6 to 16.0 mm (mean 10.9 ± 2.9 mm). The remaining lesion

Please cite this article in press as: Maruyama H, et al. Changes in tumor vascularity precede microbubble contrast accumulation deficit in the process of dedifferentiation of hepatocellular carcinoma. Eur J Radiol (2009), doi:10.1016/j.ejrad.2009.08.017

Table 1
Pathological results and contrast enhancement of hepatocellular carcinoma.

Case	Size (mm)	Pathology I/O	Inner nodule		Outer nodule	
			V	L	V	L
1	24	M/W[a]	Hyper	Hypo	Hypo	Iso
2	14.4	W	Hyper	Hypo	Hypo	Iso
3	23	W	Hyper	Iso	Hypo	Iso
4	39	M/W[b]	Hyper	Hypo	Hypo	Iso
5	25.1	W	Hyper	Hypo	Hypo	Iso
6	17.1	W	Hyper	Hypo	Hyper	Hypo
7	34.3	M	Hyper	Hypo	Iso	Iso
8	24.8	W	Hyper	Hypo	Hyper	Hypo
9	28.5	W	Hyper	Iso	Iso	Iso
10	31.1	M/W[a]	Hyper	Hypo	Hyper	Hypo

I/O: Inner nodule/outer nodule, V: vascular phase, L: late phase, W: well differentiated HCC, M: moderately differentiated HCC, Hyper: hyper-enhancement, Iso: iso-enhancement, Hypo: hypo-enhancement.
[a] Separate sampling for inner and outer nodules by needle biopsy.
[b] Assessment of pathological result on surgically resected specimen.

showed a hypoechoic appearance without any difference between the outer and inner nodules. Neither US nor contrast-enhanced CT detected ascites, vascular abnormality, portal vein thrombosis, or portal vein tumor thrombosis.

3.2. Contrast-enhanced US findings in HCC

Vascular-phase US images of the inner nodule were hyper-enhanced in appearance in all 10 lesions, and images of the outer nodule were hyper-enhanced in 3 lesions, iso-enhanced in 2, and hypo-enhanced in 5 (Table 1). As the contrast enhancement of the inner nodule was much stronger than that of the outer nodule in all lesions, dedifferentiation of the tumor was clearly demonstrated in this vascular phase. Late-phase images of the inner nodule showed a hypo-enhanced appearance in 8 lesions and iso-enhancement in 2. Meanwhile, late-phase images of the outer nodule were iso-enhanced in the 7 lesions that showed an iso- or hypo-enhanced appearance in the vascular phase, and hypo-enhanced in the 3 showing a hyper-enhanced appearance in the vascular phase (Tables 1 and 2 and Figs. 1 and 2). Neither the inner nodules nor the outer nodules had a hyper-enhanced appearance in the late phase. A late-phase hypo-enhanced appearance was significantly more frequent in the nodules showing early-phase hyper-enhancement (11/13) than in the nodules showing early-phase iso- or hypo-enhancement (0/7) in both the inner and outer nodules.

3.3. Pathological results and contrast enhancement in each nodule

Pathological examination of the 7 HCC lesions without separate nodule sampling revealed well-differentiated HCC in 6 lesions and moderately differentiated HCC in one. The remaining 3 lesions showed well-differentiated HCC in the outer nodule and moderately differentiated HCC in the inner nodule. Upon contrast-enhanced US, all inner nodules in the latter 3 lesions showed a hyper-enhanced appearance in the vascular phase and hypo-enhancement in the late phase. On the other hand, the outer nodule in 2 lesions showed a hypo-enhanced appearance in the vascular phase and iso-enhancement in the late phase, and that in one lesion showed a hyper-enhanced appearance in the vascular phase and hypo-enhancement in the late phase.

Table 2
Contrast enhancement in the outer and inner nodule.

	Vascular phase (Hyper/Iso/Hypo)	Late phase (Hyper/Iso/Hypo)
Outer nodule	3/2/5	0/7/3
Inner nodule	10/0/0	0/2/8

Hyper: Hyper-enhancement, Iso: iso-enhancement, Hypo: hypo-enhancement.

4. Discussion

The nodule-in-nodule appearance of HCC lesions, supported by radiological and pathological evidence, represents a characteristic feature of developing HCC [15–21]. Typical findings on contrast-enhanced CT/magnetic resonance imaging include a hypervascular spot within the iso- or hypo-vascular lesion. The outer nodule is generally considered to be at an earlier stage of carcinogenesis relative to the inner nodule in HCC, hence the nodule-in-nodule appearance.

A cardinal non-contrast US finding in HCC lesions with a nodule-in-nodule appearance is a hypoechoic nodule within a hyperechoic nodule, which was also the most common pattern in our study. However, as previously reported, focal hepatic lesions with nodule-in-nodule appearance show various patterns on the grey-scale sonogram, and one lesion in the current study appeared hypoechoic without showing any difference between the inner and outer nodules [23]. Therefore, hemodynamic-based imaging may be required to diagnose nodule-in-nodule-appearing tumors, and vascular-phase sonograms can be obtained easily with Sonazoid and have clearly demonstrated the difference in vascularity between the inner and outer nodules in HCC lesions, as in contrast-enhanced CT images. Similar to the results from previous studies using other kinds of microbubble contrast agents, the current study suggested that contrast-enhanced US with Sonazoid can offer at least the same rate of detecting characteristic HCC tumor vascularity as contrast-enhanced CT [24–26].

Late-phase appearance varied in the inner nodule, with 80% of nodules showing a hypo-enhanced appearance and 20% of nodules showing iso-enhancement. These results may be absolutely reasonable because late-phase wash-out following vascular-phase hyper-enhancement is considered to be typical findings in cases of HCC [11,12]. Meanwhile, outer nodules that were hypo- or iso-enhanced in the vascular phase showed an iso-enhanced appearance in the late phase, and those hyper-enhanced in the vascular phase showed hypo-enhancement in the late phase. As the inner nodule appears to be in the post-dedifferentiated state and thus in a more advanced stage of carcinogenesis relative to the outer nodule, it is logical to assume that, as HCC progresses, the inner nodule may eventually exhibit the same enhancement pattern seen later in the outer nodule. Thus, our results suggest that tumor neovascularity precedes the deficit in microbubble contrast accumulation during the dedifferentiation process of HCC. In fact, it is strongly speculated that developing HCC progresses from lesions with hypo- or iso-enhancement in the vascular phase and iso-enhancement in the late phase, to lesions with hyper-enhancement in the vascular phase and iso-enhancement in the late phase, and subsequently to lesions with hyper-enhancement in the vascular phase and hypo-enhancement in the late phase. Therefore, a late-phase observation alone may not always be sufficient in screening for HCC because it could fail to detect developing HCC with an iso-enhanced appearance in the late phase.

Phagocytosis of microbubbles by Kupffer cells is one of the theoretical mechanisms for the late-phase enhancement findings in contrast-enhanced US with Sonazoid [14]. Considering the relationship between Kupffer cell distribution and cellular differentiation in HCC, the microbubble-related enhancement patterns in the late phase in our study might be explained by this theory [5,6]. The Levovist contrast agent also accumulates in the liver, and it is

Please cite this article in press as: Maruyama H, et al. Changes in tumor vascularity precede microbubble contrast accumulation deficit in the process of dedifferentiation of hepatocellular carcinoma. Eur J Radiol (2009), doi:10.1016/j.ejrad.2009.08.017

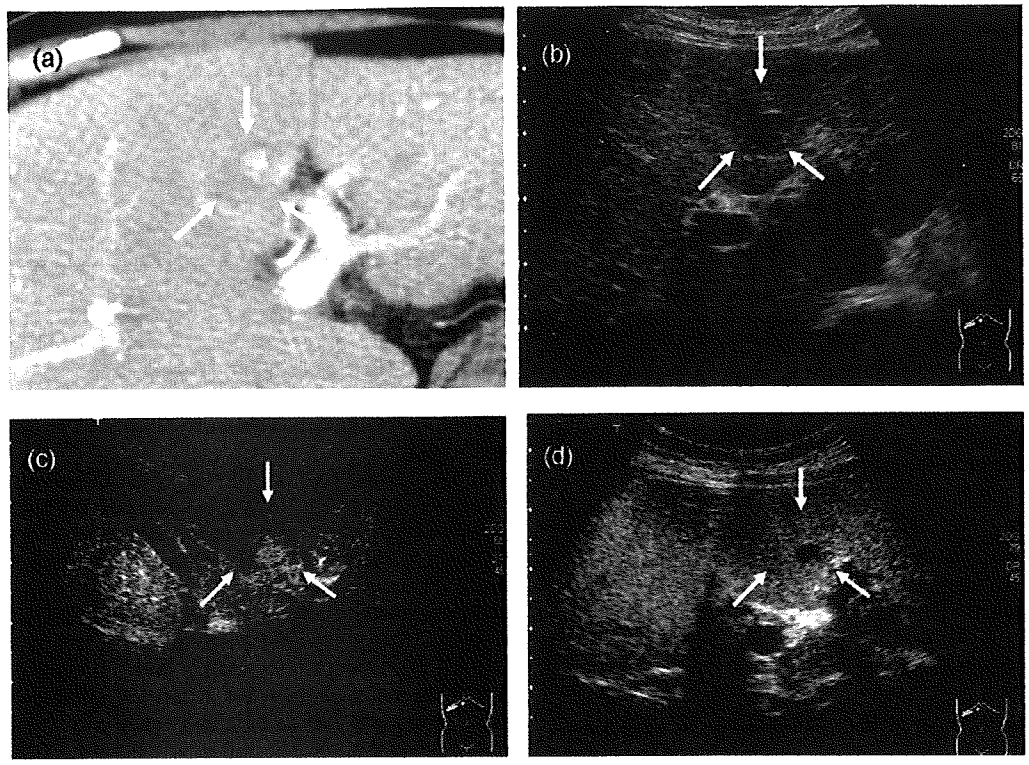

Fig. 1. A 69-year-old female, hepatitis C virus-related cirrhosis, HCC with nodule-in-nodule appearance (S4, 24 mm; case 1). (a) Contrast-enhanced CT, artery-dominant phase. HCC with hypovascular outer nodule and hypervascular inner nodule (arrows). (b) Grey-scale US. HCC with hypoechoic appearance (arrows). (c) Contrast-enhanced US, vascular phase. HCC with hypo-enhanced outer nodule and hyper-enhanced inner nodule (arrows). (d) Contrast-enhanced US, late phase. HCC with iso-enhanced outer nodule and hypo-enhanced inner nodule (arrows).

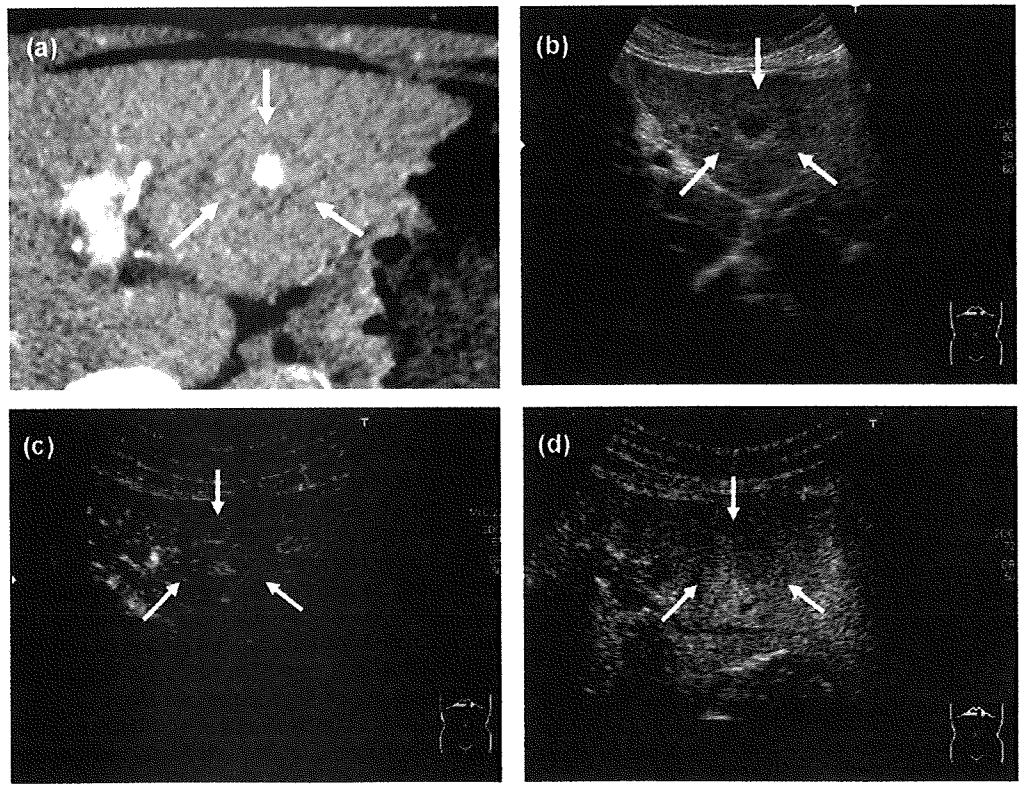

Fig. 2. A 74-year-old female, hepatitis C virus-related cirrhosis, HCC with nodule-in-nodule appearance (S3, 28.5 mm; case 9). (a) Contrast-enhanced CT, artery-dominant phase. HCC with isovascular outer nodule and hypervascular inner nodule (arrows). (b) Grey-scale US. HCC with hyperechoic outer nodule and hypoechoic inner nodule (arrows). (c) Contrast-enhanced US, vascular phase. HCC with iso-enhanced outer nodule and hyper-enhanced inner nodule (arrows). (d) Contrast-enhanced US, late phase. HCC with iso-enhanced outer and inner nodules (arrows).

Please cite this article in press as: Maruyama H, et al. Changes in tumor vascularity precede microbubble contrast accumulation deficit in the process of dedifferentiation of hepatocellular carcinoma. Eur J Radiol (2009), doi:10.1016/j.ejrad.2009.08.017

reported that late-phase enhancement with this agent in well-differentiated HCC and benign regenerative nodules was similar to that in adjacent non-tumor liver parenchyma, whereas moderately differentiated HCC tended to have a washed-out appearance in this phase [11,12,27]. Meanwhile, in studies using the contrast agents SonoVue® (Bracco, Milan, Italy) and Definity® (Lantheus, North Billerica, MA, USA), which do not accumulate in the liver, hypo-enhancement or a washed-out appearance after the vascular-phase peak enhancement and an earlier wash-out were frequent and consistent with the degree of tumor differentiation in HCC [28,29]. These results with different contrast agents suggest that hypo-enhancement or wash-out findings may be common in spite of the type of US contrast agent used, and mechanisms other than Kupffer cell distribution might account for the late-phase enhancement pattern in HCC. However, as these possible explanations are still at a speculative level, further investigations are required to account for these findings.

Our study had several limitations. The first is that the histological results of all but one HCC were obtained from specimens obtained by percutaneous US-guided needle biopsy, and separate sampling from inner and outer nodules was performed in only 2 of the 9 HCC lesions biopsied. According to previous studies, the histological structure of the outer nodule in nodule-in-nodule-appearing lesions varies and can be diagnosed as: adenomatous hyperplasia, siderotic regenerative nodule, macroregenerative nodule, or well-differentiated HCC [15–19]. Assessment of the pathology of the surgically resected specimen might allow confirmation of agreement between the histological findings and the results of US with contrast enhancement. The second limitation is that our study consisted of a small number of subjects and lacked follow-up of the natural progression of HCC with nodule-in-nodule appearance. Further studies with large numbers of patients and with US follow-up of contrast-enhanced changes in each nodule during the period between diagnosis and treatment may be necessary to allow us to draw more definitive conclusions.

5. Conclusions

Dedifferentiation of HCC may be accompanied by changes in neovascularity prior to the reduction in microbubble contrast accumulation, with the latter possibly related to Kupffer cell distribution. Although late-phase ultrasonography with static microbubbles may have the advantage of easy and stable observation, vascular-phase contrast enhancement using Sonazoid dynamic microbubbles could allow early recognition of the dedifferentiation of HCC.

References

[1] Bosch FX, Ribes J, Borras J. Epidermiology of primary liver cancer. Semin Liver Dis 1999;19(3):271–85.
[2] Okuda K. Hepatocellular carcinoma. J Hepatol 2000;32(1 Suppl.):225–37.
[3] Tong MJ, Blatt LM, Kao VW. Surveillance for hepatocellular carcinoma in patients with chronic viral hepatitis in the United States of America. J Gastroenterol Hepatol 2001;16(7):553–9.
[4] Larcos G, Sorokopud H, Berry G, Farrell GC. Sonographic screening for hepatocellular carcinoma in patients with chronic hepatitis or cirrhosis: an evaluation. AJR Am J Roentgenol 1998;171(2):433–5.
[5] Tanaka M, Nakashima O, Wada Y, Kage M, Kojiro M. Pathomorphological study of Kuppfer cells in hepatocellular carcinoma and hyperplastic nodular lesions in the liver. Hepatology 1996;24(4):807–12.
[6] Imai Y, Murakami T, Yoshida S, et al. Super paramagnetic iron oxide enhanced magnetic resonance images of hepatocellular carcinoma: correlation with histological grading. Hepatology 2000;32(2):205–12.
[7] Hayashi M, Matsui O, Ueda K, et al. Correlation between the blood supply and grade of malignancy of hepatocellular nodules associated with liver cirrhosis: evaluation by CT during intraarterial injection of contrast medium. Am J Roentgenol 1999;172(4):969–76.
[8] Kremkau FW. Diagnostic ultrasound: principles and instruments. 4th ed. Philadelphia: WB Saunders; 1993.
[9] Mitchell DG. Color Doppler imaging: principles, limitations, and artifacts. Radiology 1990;177(1):1–10.
[10] Goldberg BB. Ultrasound contrast agents. Martin Dunitz Ltd.; 1997.
[11] Rettenbacher T. Focal liver lesions: role of contrast-enhanced ultrasound. Eur J Radiol 2007;64(2):173–82.
[12] Quaia E. Microbubble ultrasound contrast agents: an update. Eur Radiol 2007;17(8):1995–2008.
[13] Marelli C. Preliminary experience with NC100100, a new ultrasound contrast agent for intravenous injection. Eur Radiol 1999;9(Suppl. 3):S343–6.
[14] Watanabe R, Matsumura M, Munemasa T, Fujimaki M, Suematsu M. Mechanism of hepatic parenchyma-specific contrast of microbubble-based contrast agent for ultrasonography: microscopic studies in rat liver. Invest Radiol 2007;42(9):643–51.
[15] Matsui O, Kadoya M, Kameyama T, et al. Adenomatous hyperplastic nodules in the cirrhotic liver: differentiation from hepatocellular carcinoma with MR imaging. Radiology 1989;173(1):123–6.
[16] Mitchell DG, Rubin R, Siegelman ES, Burk Jr DL, Rifkin MD. Hepatocellular carcinoma within siderotic regenerative nodules: appearance as a nodule within a nodule on MR images. Radiology 1991;178(1):101–3.
[17] Muramatsu Y, Nawano S, Takayasu K, et al. Early hepatocellular carcinoma: MR imaging. Radiology 1991;181(1):209–13.
[18] Winter 3rd TC, Takayasu K, Muramatsu Y, et al. Early advanced hepatocellular carcinoma: evaluation of CT and MR appearance with pathologic correlation. Radiology 1994;192(2):379–87.
[19] Sadek AG, Mitchell DG, Siegelman ES, Outwater EK, Matteucci T, Hann HW. Early Hepatocellular carcinoma that develops within macroregenerative nodules: growth rate depicted at serial MR imaging. Radiology 1995;195(3):753–6.
[20] Kojiro M. 'Nodule-in-nodule' appearance in hepatocellular carcinoma: its significance as a morphologic marker of dedifferentiation. Intervirology 2004;47(3–5):179–83.
[21] Zheng RQ, Zhou P, Kudo M. Hepatocellular carcinoma with nodule-in-nodule appearance: demonstration by contrast-enhanced coded phase inversion harmonic imaging. Intervirology 2004;47(3–5):184–90.
[22] Maruyama H, Takahashi M, Ishibashi H, et al. Ultrasound-guided treatments under low acoustic power contrast harmonic imaging for hepatocellular carcinomas undetected by B-mode ultrasonography. Liver Int 2009;29(5):708–14.
[23] Ishida Y, Nagamatsu H, Koga H, Yoshida H, Kojiro M, Sata M. Hepatocellular carcinoma with a "nodule-in-nodule" appearance reflecting an unusual dilated pseudoglandular structure. Int Med 2008;47(13):1215–8.
[24] Numata K, Tanaka K, Kiba T, et al. Contrast-enhanced, wide-band harmonic gray scale imaging of hepatocellular carcinoma. Correlation with helical computed tomographic findings. J Ultrasound Med 2001;20(2):89–98.
[25] Giorgio A, Ferraioli G, Tarantino L, et al. Contrast-enhanced sonographic appearance of hepatocellular carcinoma in patients with cirrhosis: comparison with contrast-enhanced helical CT appearance. AJR Am J Roentgenol 2004;183(5):1319–26.
[26] Bolondi L, Gaiani S, Celli N, et al. Characterization of small nodules in cirrhosis by assessment of vascularity: the problem of hypovascular hepatocellular carcinoma. Hepatology 2005;42(1):27–34.
[27] Yoshizumi H, Maruyama H, Okugawa H, et al. How to characterize non-hypervascular hepatic nodules on contrast-enhanced computed tomography in chronic liver disease: feasibility of contrast-enhanced ultrasound with a microbubble contrast agent. J Gastroenterol Hepatol 2008;23(10):1528–34.
[28] Nicolau C, Catalá V, Vilana R, et al. Evaluation of hepatocellular carcinoma using SonoVue, a second generation ultrasound contrast agent: correlation with cellular differentiation. Eur Radiol 2004;14(6):1092–9.
[29] Jang HJ, Kim TK, Burns PN, Wilson SR. Enhancement pattern of hepatocellular carcinoma at contrast-enhanced US: comparison with histologic differentiation. Radiology 2007;244(3):898–906.

Please cite this article in press as: Maruyama H, et al. Changes in tumor vascularity precede microbubble contrast accumulation deficit in the process of dedifferentiation of hepatocellular carcinoma. Eur J Radiol (2009), doi:10.1016/j.ejrad.2009.08.017

Human Pathology (2009) 40, 1304–1311

ELSEVIER

Human
PATHOLOGY

www.elsevier.com/locate/humpath

Original contribution

Distinct expression of polycomb group proteins EZH2 and BMI1 in hepatocellular carcinoma

Yutaka Yonemitsu[a], Fumio Imazeki[a], Tetsuhiro Chiba[b], Kenichi Fukai[a], Yuichiro Nagai[c], Satoru Miyagi[b], Makoto Arai[a], Ryutaro Aoki[a], Masaru Miyazaki[d], Yukio Nakatani[e], Atsushi Iwama[b], Osamu Yokosuka[a,*]

[a]*Department of Medicine and Clinical Oncology, Graduate School of Medicine, Chiba University, Chiba 260-8670, Japan*
[b]*Department of Cellular and Molecular Medicine, Graduate School of Medicine, Chiba University, Chiba 260-8670, Japan*
[c]*Department of Molecular Pathology, Graduate School of Medicine, Chiba University, Chiba 260-8670, Japan*
[d]*Department of General Surgery, Graduate School of Medicine, Chiba University, Chiba 260-8670, Japan*
[e]*Department of Basic Pathology, Graduate School of Medicine, Chiba University, Chiba 260-8670, Japan*

Received 2 August 2008; revised 20 January 2009; accepted 30 January 2009

Keywords:
EZH2;
BMI1;
Hepatocellular carcinoma;
Short hairpin RNA;
MTS assay

Summary Polycomb gene products play a crucial role in the development of highly malignant phenotypes and aggressive cancer progression in a variety of cancers; however, their role in hepatocellular carcinoma remains unclear. First, we analyzed the impact of EZH2 and BMI1 modulation on cell growth of HepG2 cells. 3-(4,5-Dimethylthiazol-2-yl)-5-(3-carboxymethoxyphenyl)-2-(4-sulfophenyl)-2*H*-tetrazolium assays revealed marked growth inhibition after *EZH2* or *BMI1* knockdown. In addition, simultaneous knockdown of these 2 genes further augmented cell growth inhibitory effects. Next, we conducted immnuohistochemical assessment of 86 hepatocellular carcinoma surgical specimens, evaluating the correlation between EZH2 and BMI1 protein expression and clinicopathologic features. High-level EZH2 and BMI1 expression was detected in 57 (66.3%) and 52 tumor tissues (60.5%), respectively. Among these, 48 tumor tissues (55.8%) showed colocalization of EZH2 and BMI1 in almost all tumor cells. The cumulative recurrence rate, but not survival rate, was significantly higher in patients positive for EZH2 ($P = .029$) and BMI1 ($P = .039$) than in their negative counterparts, as determined by Kaplan-Meier analysis. These data indicate that EZH2 and BMI1 may cooperate in initiation and progression of hepatocellular carcinoma.

1. Introduction

Cell-type–specific gene expression profiles are stabilized by changes in chromatin structure and DNA methylation patterns. Polycomb group proteins form multiprotein complexes and serve as a cellular memory system through epigenetic chromatin modifications [1,2]. So far, 2 major polycomb group complexes have been well characterized. Polycomb repressive complex 1 includes BMI1, RNF110/MEL18, HPH, CBX2/HPC1, Ring1A, and Rind1B, and polycomb repressive complex 2 includes EED, EZH2, and SUZ12. The polycomb repressive complex 1 and polycomb repressive complex 2 possess H2A-K119 ubiquitin E3 ligase activity and H3-K27 methyltransferase activity, respectively. BMI1, which is part of the polycomb repressive complex 1, contributes to the enhancement of RING1-mediated H2A-K119 ubiquitin E3 ligase activity. EZH2, a key molecule of

* Corresponding author.
E-mail address: yokosukao@faculty.chiba-u.jp (O. Yokosuka).

0046-8177/$ – see front matter © 2009 Elsevier Inc. All rights reserved.
doi:10.1016/j.humpath.2009.01.017

polycomb repressive complex 2, possesses histone methyltransferase activity and causes methylation at lysine residues of histone H3 (H3-K27). Both histone modifications contribute to polycomb group gene silencing. Although no physical associations have been demonstrated between the 2 complexes, H3-K27 methylation serves as a binding site for the recruitment of the polycomb repressive complex 1. Thus, the 2 polycomb group complexes could function in a cooperative manner to maintain gene silencing [1,2].

Polycomb repressive complex 1 has been implicated in stem cell self-renewal [1,2], a process by which epigenetic cellular memory is precisely inherited by daughter cells through cell division. Among polycomb repressive complex 1 components, we have demonstrated that BMI1 plays a central role in the inheritance of self-renewal of hematopoietic stem cells in both loss-of-function and gain-of-function analyses [3]. It is well recognized that polycomb repressive complex 1 transcriptionally represses tumor suppressor genes such as the Ink4b-Arf-Ink4a locus, which functions as a barrier to eliminate oncogenic cells by triggering apoptosis or cellular senescence [1,4]. We have demonstrated that tight repression of Ink4a-Arf in hematopoietic stem cells is essential to maintain the self-renewing capacity of hematopoietic stem cells [5]. On the other hand, there is increasing evidence that up-regulation of polycomb group proteins is deeply involved in tumor development. EZH2 is reportedly involved in the pathogenesis of malignant lymphoma and multiple myeloma [6,7]. BMI1 was initially identified as a c-myc–cooperating protooncogene in murine lymphomas [8], and increased levels of BMI1 expression has been implicated not only in human lymphoma but also in several types of leukemia [9-11]. Moreover, coexpression of EZH2 and BMI1 appears to be associated with the degree of malignancy in B-cell non–Hodgkin lymphoma [12]. Of importance, recent studies demonstrated that the increased expression of EZH2 proteins correlates with progression and poor prognosis of solid tumors such as prostate cancer and breast cancer [13-15].

In the present study, we first examined the cell growth activity of hepatocellular carcinoma cells stably expressing short hairpin RNAs against EZH2 and BMI1 in culture. Next, we conducted immunohistochemical analyses to estimate the expression levels of polycomb group proteins EZH2 and BMI1 in hepatocellular carcinoma. The cumulative survival rates and recurrent rates were analyzed using the Kaplan-Meier method to ask whether these molecules could be novel biologic markers.

2. Materials and methods

2.1. Cell culture

The hepatocellular carcinoma cell line HepG2 was cultured in Dulbecco's modified Eagle's medium (Invitrogen Life Technologies, Carlsbad, CA) supplemented with 10% fetal bovine serum and 1% penicillin/streptomycin (Invitrogen).

2.2. Lentiviral production and transduction

Lentiviral vectors (CS-H1-short hairpin RNA EF-1α-EGFP and CS-CDF-RfA-ERP) expressing short hairpin RNA that targets human EZH2 (target sequence: 5′-GGAAAGAACGGAAATCTTA-3′), human BMI1 (target sequence: 5′-GAGAAGGAATGGTCCACTT-3′), and luciferase were constructed. Recombinant lentiviruses were produced as described elsewhere [3]. The cells were transduced with viruses in the presence of protamine sulfate.

2.3. Immunocytochemical analyses

HepG2 cells were fixed with methanol. After blocking in 10% goat serum, the cells were stained with a primary rabbit anti-EZH2 antibody (Zymed, San Francisco, CA) and a primary mouse anti-BMI1 antibody (Upstate Biotechnology, Lake Placid, NY) for 12 hours at 4°C. The cells then were washed and incubated with Alexa-555–conjugated goat anti-rabbit immunoglobulin G (IgG) (Molecular Probes, Eugene, OR) or Alexa-488–conjugated goat anti-mouse IgG (Molecular Probes), as appropriate, for 2 hours at room temperature. After being washed in phosphate-buffered saline (PBS), the cells were coverslipped with a mounting medium containing 4′,6-diamidino-2-phenylindole (DAPI) dihydrochloride (Vector Laboratories, Burlingame, CA).

2.4. Measurement of cell proliferation by 3-(4,5-dimethylthiazol-2-yl)-5-(3-carboxymethoxyphenyl)-2-(4-sulfophenyl)-2H-tetrazolium assay

Cell growth of HepG2 cells after stable knockdown of EZH2 and/or BMI1 was measured by 3-(4,5-dimethylthiazol-2-yl)-5-(3-carboxymethoxyphenyl)-2-(4-sulfophenyl)-2H-tetrazolium (MTS) assay. For this, we seeded cells in a 6-well plate at a density of 1×10^4 cells per well. MTS assays were performed in triplicate using the Cell Titer 96 Aqueous One Solution Cell Proliferation kit (Promega, Madison, WI) at culture days 2, 3, 4, and 5.

2.5. Patients and surgical specimens

Eighty-six patients who underwent surgical resection for hepatocellular carcinoma at Chiba University, Chiba, Japan, hospital were analyzed in this study. Informed consent for research use of the specimens was obtained for all cases. There were 73 male patients and 13 female patients with an average age of 63 ± 11 years (52-80 years). Among these, 32 cases had liver cirrhosis and 50 cases showed chronic hepatitis with mild to moderate activities. Liver damage of the patients was due to autoimmune disorder (n = 1), hepatitis B virus (HBV) (n = 19), hepatitis C virus (HCV)